U. S. ARMY
TRANSPORTATION RESEARCH COMMAND
FORT EUSTIS, VIRGINIA

TRECOM TECHNICAL REPORT 64-43

EFFECTS OF TRANSPIRATION THROUGH ANGLED SLOTS ON THE DEVELOPMENT OF THE TURBULENT BOUNDARY LAYER

AD-607657

Task 1D121401A14203
Contract DA 44-177-AMC-892(T)

September 1964

PROPERTY OF U. S. ARMY
TECHNICAL LIBRARY

prepared by:

MISSISSIPPI STATE UNIVERSITY
The Aerophysics Department
State College, Mississippi

NOV 16 1964

DISCLAIMER NOTICE

When Government drawings, specifications, or other data are used for any purpose other than in connection with a definitely related Government procurement operation, the United States Government thereby incurs no responsibility nor any obligation whatsoever; and the fact that the Government may have formulated, furnished, or in any way supplied the said drawings, specifications, or other data is not to be regarded by implication or otherwise as in any manner licensing the holder or any other person or corporation, or conveying any rights or permission, to manufacture, use, or sell any patented invention that may in any way be related thereto.

* * *

DDC AVAILABILITY NOTICE

Qualified requesters may obtain copies of this report from

Defense Documentation Center
Cameron Station
Alexandria, Virginia 22314

* * *

This report has been released to the Office of Technical Services, U. S. Department of Commerce, Washington 25, D. C., for sale to the general public.

* * *

Reproduction of this document in whole or in part is prohibited except with the specific written permission of the Commanding Officer, U. S. Army Transportation Research Command.

* * *

The information contained herein will not be used for advertising purposes.

* * *

The findings and recommendations contained in this repor. are those of the contractor and do not necessarily reflect the views of the U. S. Army Mobility Command, the U. S. Army Materiel Command, or the Department of the Army.

HEADQUARTERS
U S ARMY TRANSPORTATION RESEARCH COMMAND
FORT EUSTIS, VIRGINIA 23604

The study presented in this report was conducted by Mr. Gordon L. Harris of the Aerophysics Department, Mississippi State University. In April 1963, this report won first place in the graduate division of the AIAA Student Competition, Southwest Region; in January 1964, it was awarded first prize in the AIAA National Competition among all regional winners, representing a total participation of 92 colleges and universities.

This report is published for the dissemination of information and stimulation of ideas.

GARY N. SMITH
Project Engineer

PAUL J. CARPENTER
Group Leader
Applied Aeronautical Engineering Group

APPROVED.

FOR THE COMMANDER:

LARRY M. HEWIN
Technical Director

Task 1D121401A14203
Contract DA 44-177-AMC-892(T)
TRECOM Technical Report 64-43
September 1964

EFFECTS OF TRANSPIRATION THROUGH ANGLED SLOTS ON THE DEVELOPMENT OF THE TURBULENT BOUNDARY LAYER

Aerophysics Research Report No. 43

Prepared by
The Aerophysics Department
Mississippi State University
State College, Mississippi

for
U. S. ARMY TRANSPORTATION RESEARCH COMMAND
FORT EUSTIS, VIRGINIA

CONTENTS

	Page
LIST OF ILLUSTRATIONS	v
SYMBOLS	vii
INTRODUCTION	1
THEORETICAL CONSIDERATIONS	2
EXPERIMENTAL INVESTIGATIONS	8
DISCUSSION OF RESULTS	11
CONCLUDING REMARKS	14
REFERENCES	15
APPENDIX	17
ILLUSTRATIONS	19
DISTRIBUTION	44

ILLUSTRATIONS

Figure		Page
1	Theoretical Model of Conditions Existing at Angled Slot	19
2	Influence of Slot Parameters upon Change of Momentum Loss Thickness Across Angled Slot	20
3	Most Effective Slot Angle to Change θ by Suction Against the Parameter Z where $Z = \frac{2v_0^2}{U_{t_1}^2 + U_{t_2}^2}$	21
4	Photograph of TG-3 Sailplane Used for the Flight Experiments	22
5	View of Test Section and Leading Edge Fairing . . .	22
6	View of Slot Pressure Chamber and Ducting	23
7	Detailed View of Test Section Showing the Slot, the Conducting Strip of Paint and the Wire Turbulence Generators	23
8	Schematic Diagram Showing General Arrangement of Experimental Apparatus	24
9	Boundary Layer Pitot-Static Traversing Mechanism . .	25
10	Multichannel Photomanometer	25
11	Typical Boundary Layer Velocity Profiles Obtained by Means of Pitot-Static Traversing Apparatus	26
12	Experimental Configurations Investigated	27
13	Geometry of Airfoil Test Section	28
14	Comparison of Two Skin Friction Relationships for the Evaluation of U_τ from the Experimental Boundary Layer Profiles	29
15	Velocity Distributions over Test Section for Various Insert Plates, $U_\infty = 49.0$ M. P. H.	30

Figure		Page
16	Effect of Transpiration on Velocity Distribution Over the Surface of the Test Section, 45° Slot . . .	31
17	Influence of Slot Flow on the Momentum Loss Thickness 25 Slot Widths Upstream of the Slot	32
18	Effect of Transpiration on the Development of the Momentum Loss Thickness θ in Case of the 45° Slot.	33
19	Development of Momentum Loss Thickness θ for Case of the 90° Slot	34
20	Development of Momentum Loss Thickness θ for Case of the 135° Slot	35
21	Failure of the Theory in Cases where Separation and Reattachment Occur Downstream of the Slot	36
22	Effect of Transpiration on Friction Velocity U_τ in Case of the 45° Slot	37
23	Effect of Transpiration on Friction Velocity U_τ in Case of the 90° Slot	38
24	Effect of Transpiration on Friction Velocity U_τ in Case of the 135° Slot	39
25	Effect of Injection on Momentum Loss Thickness at Extreme Slot Angles	40
26	Effect of Suction on Momentum Loss Thickness at Extreme Slot Angles	41
27	Effect of Transpiration on Friction Velocity U_τ in Case of 179° Slot	42
28	Diagram of Conditions Existing in Vicinity of Extreme Angled Slot	43

LIST OF SYMBOLS

h	height of control volume, feet
H	boundary layer form parameter
L	length of slot, feet
P	total pressure, pounds per (foot)^2
p	static pressure, pounds per (foot)^2
Q_s	slot quantity flow, $Q_s = v_o w$, (feet)^2 per second
s	distance measured along surface, feet
S	total length of surface used for testing, S = 2.16 feet
U	potential velocity at edge of boundary layer, feet per second
u	s - component of velocity at point y in boundary layer, feet per second
U_τ	friction velocity $U_\tau = \sqrt{\frac{\tau}{\rho}}$, feet per second
v_o	mean velocity across the slot, feet per second
v_e	y - component of velocity at edge of boundary layer, feet per second
w	slot width, feet
w'	$w' = \frac{w}{\sin\sigma}$, feet
y	distance measured from surface in direction normal to surface, feet
Z	parameter $Z = \frac{2v_1^2}{U_{\tau_1}^2 + U_{\tau_2}^2}$
δ^*	displacement thickness $\delta^* = \int (1 - \frac{u}{U})\, dy$, feet
θ	momentum thickness $\theta = \int_0^\infty \frac{u}{U}(1 - \frac{u}{U})\, dy$ feet
ρ	density, pounds (second)^2 per (foot)^4
ν	kinematic viscosity, (feet)^2 per second

σ slot angle, degrees

τ shearing stress, pounds per $(\text{foot})^2$

Subscripts

∞ Denotes free stream condition

o Denotes condition at surface

b Denotes condition at base of control volume

1 Denotes condition at upstream edge of slot

2 Denotes condition at downstream edge of slot

i Denotes initial conditions

INTRODUCTION

Much has been written in recent years concerning boundary layer control for both high lift and low drag by means of distributed and slot transpiration. While considerable energy has been devoted to the fundamental examination of the effects of distributed transpiration on both the laminar and turbulent boundary layers, slot studies tend almost exclusively toward aerodynamic evaluations of particular body shapes utilizing slots for improved performance (References 1 and 2). While this is a convenient preliminary criterion of slot effectiveness, it does not provide a means by which the effect of slot transpiration in the most general case may be predicted.

In addition, it is of interest to examine the case of suction and injection at an arbitrary angle to the surface and to compare this with normal transpiration. Two areas in which this may find application are: (1) the low-shear turbulent boundary layer (Reference 3) where angled slot injection may be effectively employed to reduce the local turbulent skin friction, and (2) suction at some angle to the surface which may be more effective than normal suction in removing the low-energy boundary layer fluid near the surface.

In this study, an attempt will be made to fundamentally understand the nature of slot transpiration and to establish an appropriate mathematical formulation of the problem suitable for its solution. These solutions will be compared with experimental data obtained at flight Reynolds numbers.

THEORETICAL CONSIDERATIONS

In the mathematical analysis, frequent use is made of the principle of relative orders of magnitude. The validity of this procedure can be verified by substituting typical numerical values into the resulting equations and noting the influence of the neglected terms upon the final results. The equations will be derived on the basis of turbulent flow; however, as pointed out in the later section, the analysis may be directly extended to laminar boundary layers under certain conditions.

The assumptions utilized in the subsequent analysis are collectively listed for convenience as follows:

a. The flow is two dimensional.

b. The fluid is incompressible.

c. The flow does not separate immediately downstream of the slot.

d. The slot opening in the surface $w' = w/\sin\sigma$ is small with respect to the characteristic length of the body under consideration.

e. Since the paramount effect of the injection on the boundary layer is the local addition of relatively large quantities of fluid, the slot velocity is taken to be a mean constant across the slot.

f. The transpiration velocity does not change the local potential velocity at the edge of the boundary layer.

g. The total effect of the transpiration takes place over the slot width; that is, the boundary layer discontinuously experiences the influence of the transpiration.

h. The change in shearing stress across the slot is linear.

i. The change in potential velocity across the slot, if any, is linear.

j. The development of the momentum loss thickness downstream of the transpiration slot is dependent only upon the initial value of θ and the velocity distribution over the surface.

The assumptions will be discussed in the light of experimental evidence in a later section.

A control volume of height h was selected across the slot as shown in Figure 1, and the net s-wise momentum transfer through the control volume balances against the friction and pressure forces.

$$\rho\int_0^h u_1^2\,dy + \rho(v_0\,\omega'\sin\sigma)\,v_0\cos\sigma - \rho\int_0^h u_2^2\,dy$$

$$-\rho v_e\,\omega'\left(\frac{U_1+U_2}{2}\right) = \int_0^{\omega'}\tau_0\,ds + (P_2-P_1)\,h\,. \tag{1}$$

The quantity flow $v_e\,\omega'$ at the upper edge of the control volume is assumed to exit with an s-direction velocity equal to the mean potential velocity across the slot, $\frac{U_1+U_2}{2}$. At the edge of the boundary layer, Bernoulli's equation may be applied

$$P_1 = P_1 - \tfrac{1}{2}\rho U_1^2$$

$$P_2 = P_2 - \tfrac{1}{2}\rho U_2^2,$$

and since the motion outside of the boundary layer is irrotational, $P_1 = P_2$, and therefore

$$P_2 - P_1 = \tfrac{1}{2}\rho(U_1^2 - U_2^2).$$

Substituting this expression into equation 1, with $\omega' = \frac{\omega}{\sin\sigma}$ and $U_\tau = \sqrt{\frac{\tau_0}{\rho}}$, the following relation ship is obtained:

$$\frac{2U_1^2}{U_1+U_2}\int_0^h\left(\frac{u_1}{U_1}\right)^2 dy + \frac{2v^2\omega\cos\sigma}{U_1+U_2} - \frac{2U_2^2}{U_1+U_2}\int_0^h\left(\frac{u_2}{U_2}\right)^2 dy$$

$$-\frac{2}{U_1+U_2}\int_0^{\omega'} U_\tau^2\,ds - (U_1-U_2)h = v_e\,\omega'. \tag{2}$$

Applying the principle of continuity to the control volume yields

$$\rho \int_0^h u_1 \, dy + \rho v_0 w' \sin\sigma - \rho \int_c^h u_2 \, dy = \rho v_e w'$$

or,

$$U_1 \int_0^h \left(\frac{u_1}{U_1}\right) dy + v_0 w - U_2 \int_0^h \left(\frac{u_2}{U_2}\right) dy = v_e w'. \tag{3}$$

Eliminating v_e between equations 2 and 3 and letting

$$\int_0^h \left(\frac{u}{U}\right)^2 dy = h - \delta^* - \theta \tag{4}$$

and

$$\int_0^h \frac{u}{U} \, dy = h - \delta^*,$$

the following relationship is obtained:

$$-\frac{2U_1^2}{U_1+U_2}(\delta_1^*+\theta_1) + \frac{2U_2^2}{U_1+U_2}(\delta_2^*+\theta_2) + \frac{2U_1^2 h}{U_1+U_2} - \frac{2U_2^2 h}{U_1+U_2}$$

$$+ \frac{2v_0^2 w \cos\sigma}{U_1+U_2} - U_1(h-\delta^*) + U_2(h-\delta_2^*) - v_0 w$$

$$= \frac{2}{U_1+U_2} \int_0^{w'} U_{v_0}^2 \, ds + (U_1 - U_2)h$$

$$\frac{2U_2^2}{U_1+U_2}(\delta_2^*+\theta_2) - \frac{2U_1^2}{U_1+U_2}(\delta_1^*+\theta_1) + U_1\delta^* - U_2\delta_2^*$$

$$= v_0 w - \frac{2v_0^2 w \cos\sigma}{U_1+U_2} + \frac{2}{U_1+U_2} \int_0^{w'} U_{v_0}^2 \, ds. \tag{5}$$

Since the change in shearing stress across the slot has been assumed to be linear,

$$\int_0^{\omega'} U_{\tau_b}^2 \, ds = \frac{\omega'}{2}\left(U_{\tau_1}^2 + U_{\tau_2}^2\right) = \frac{\omega}{2\sin\sigma}\left(U_{\tau_1}^2 + U_{\tau_2}^2\right). \tag{6}$$

Substituting equation 6 in equation 5, letting $\delta^* = H\theta$, and solving for θ_2 yields the expression

$$\theta_2 = \frac{2U_1^2(H_1+1)\theta_1 - (U_1+U_2)U_1 H_1 \theta_1 + (U_1+U_2)v_0\omega - 2v_0^2\omega\cos\sigma + \frac{\omega}{\sin\sigma}\left(U_{\tau_1}^2 + U_{\tau_2}^2\right)}{2U_2^2(H_2+1) - U_2 H_2 (U_1+U_2)}. \tag{7}$$

In most applications the change in potential velocity over the slot may be neglected so that $U_1 = U_2 = U$ and

$$\theta_2 = \theta_1 + \frac{v_0}{U}\omega\left(1 - \frac{v_0}{U}\cos\sigma\right) + \frac{\omega}{2\sin\sigma}\left[\left(\frac{U_{\tau_1}}{U}\right)^2 + \left(\frac{U_{\tau_2}}{U}\right)^2\right]. \tag{8}$$

Equations 7 and 8 may be used to solve for the momentum loss thickness at the downstream edge of the slot provided that auxiliary expressions relating θ_2, H_2 and U_{τ_2} may be found at this point. The term $\frac{\omega}{2\sin\sigma}\left[\left(\frac{U_{\tau_1}}{U}\right)^2 + \left(\frac{U_{\tau_2}}{U}\right)^2\right]$ in equation 8 is of a lower order of magnitude than the other terms in the equation in cases of injection and moderate suction quantities, indicating that the variation of U_{τ_2} within reasonably wide limits has a negligible effect upon the value of θ_2. In view of this, letting $U_{\tau_1} = U_{\tau_2}$ would not create a significant error. In fact, for rapid approximate calculations this term may be ignored entirely, giving the simple expression

$$\theta_2 = \theta_1 + \frac{v_0}{U}\omega\left(1 - \frac{v_0}{U}\cos\sigma\right), \tag{9}$$

which is plotted in Figure 2. In the case where the suction quantity is sufficient to appreciably reduce the boundary layer thickness, U_{τ_2} may attain such high values that the term $\left(\frac{U_{\tau_2}}{U}\right)^2$ in equation 8 would become significant, and the above hypothesis would no longer be valid.

It has been assumed that the development of θ is a function of θ_2 and the velocity distribution downstream of the slot, and therefore, any of the presently acceptable procedures for calculating the

momentum loss thickness on an impervious surface in an arbitrary pressure gradient may be employed. In the present analysis, the method of Von Doenhoff and Tetervin as outlined in Appendix 1 was employed.

At any point downstream of the slot, the momentum integral equation for an impervious surface

$$U_\tau = U\sqrt{\frac{d\theta}{ds} + (H+2)\frac{\theta}{U}\frac{dU}{ds}} \tag{10}$$

may be applied since the quantities θ, U, $\frac{d\theta}{ds}$ and $\frac{dU}{ds}$ are known at any position from the foregoing considerations. The value of $(H+2)$ is not greatly affected by any change in the value of H within the limits $H=1.2$ to $H=1.8$ where U_τ is comparatively insensitive to the variation of H. Values of $H>1.8$ are associated with turbulent boundary layers approaching separation, a condition which can exist only a short distance downstream of the slot because of the highly turbulent entrainment region immediately aft of the injection slot which tends to reduce H to within the normal range of an attached turbulent boundary layer. It would therefore appear that the use of a mean value of $H=1.5$ in equation 10 would not create any significant error. The errors resulting from this approximation are probably of a lower order of magnitude than those incurred in measuring $\frac{d\theta}{ds}$ and $\frac{dU}{ds}$ where a small discrepancy in either of these slopes would appreciably affect the value of U_τ.

The method for calculating the effect of a transpiration slot on the development of a turbulent boundary layer is briefly outlined in the following step-by-step procedure:

1. Obtain velocity or pressure distribution over the surface, either from potential flow theory or from experiment.

2. Calculate the development of the turbulent boundary layer up to the position of the slot by a suitable method (for example, Reference 5).

3. Apply equation 8 or 9, depending on the accuracy required to obtain the change in θ across the slot.

4. Utilizing this new initial value of θ, calculate the development of θ behind the slot.

5. Equation 11 may now be employed at desired positions to obtain U_τ.

Equation 8 indicates that the optimum value of σ for decreasing θ lies between 0 and $\frac{\pi}{2}$ and is a function of the quantities v_0, v_{τ_1}, and v_{τ_2}. Although little error may be expected to accrue from applying equation 9 to calculating θ growth, substantial disagreement is introduced in solving it for the optimum angle $\sigma_{\Delta\theta MAX}$ since the approximate equation fails as the limit $\frac{\partial \Delta\theta}{\partial \sigma} = 0$ is approached. Therefore, in applying the maximum value principle to obtain $\sigma_{\Delta\theta MAX}$, the complete relationship must be employed.

$$\frac{\partial \Delta\theta}{\partial \sigma} = \frac{\partial}{\partial \sigma}\left\{\frac{v_0}{U}\omega\left(1 - \frac{v_0}{U}\cos\sigma\right) + \frac{1}{2}\frac{\omega}{\sin\sigma}\left[\left(\frac{v_{\tau_1}}{U}\right)^2 + \left(\frac{v_{\tau_2}}{U}\right)^2\right]\right\}$$

$$= \left(\frac{v_0}{U}\right)^2 \omega \sin\sigma - \frac{1}{2}\frac{\cos\sigma}{\sin^2\sigma}\omega\left[\left(\frac{v_{\tau_1}}{U}\right)^2 + \left(\frac{v_{\tau_2}}{U}\right)^2\right] = 0$$

or

$$\frac{\cos\sigma_{\Delta\theta MAX}}{\sin^3\sigma_{\Delta\theta MAX}} = \frac{2v_0^2}{v_{\tau_1}^2 + v_{\tau_2}^2} = L .$$

This equation is shown plotted in Figure 3, and $\sigma_{\Delta\theta MAX}$ is seen to lie between 0 and $\frac{\pi}{2}$. It should be noted that this may not, however, correspond to the most efficient suction angle from the standpoint of blower power required, since other considerations such as slot shape may conflict with this result.

EXPERIMENTAL INVESTIGATIONS

The experiments were performed on a test section which was mounted on the starboard wing of a TG-3 sailplane (Figures 4 and 5). The section was designed to provide a plane-surfaced testing area upstream and downstream of the slot location. The boundary layer was found to be attached at all points on the section, and the large end plates rendered the flow two dimensional. The handling characteristics of the sailplane were not adversely affected by the installation. The test section was constructed of mahogany plywood, primed and covered with numerous coats of aircraft dope and smoothed to a fine finish. The slots were milled in 1/4-inch steel plates which fitted into a rectangular duct in the test section as shown in Figures 6 and 7, and by changing the plates, the angle of the slot could be varied. The flow was rendered turbulent before impingement upon the test section by means of parallel steel wires placed in the region of the stagnation streamline. The power source for the transpiration slot was a 350-cubic-feet-per-minute axial-drive electric blower, the speed of which could be varied by means of two rheostats, thereby regulating the slot velocity to within 0.20 foot per second. The blower was powered by a 24-volt battery, which, in turn, was charged periodically in flight by a 2.5-hp. gasoline auxiliary power unit located between the pilot and observer cockpits. The general arrangement of the experimental apparatus is illustrated in Figure 8. The wiring, ducting and tubing were channeled along the leading edge into the fuselage and completely covered by an aluminum fairing to reduce possible tailplane buffet which would result from the otherwise separated flow region near the wing root. The slot velocity was obtained indirectly by means of internal chamber pressure taps calibrated against the local static pressure at the slot. The calibration was performed under static conditions by measuring the quantity flow through the slot resulting from a given pressure differential across it. The boundary layer velocity profiles were measured by a traversing Pitot-static system mounted on a calibrated micrometer screw. The instrument was electrically operated, and repeatable "y"-values were obtained to the nearest 0.001 inch (Figure 9). A chordwise strip of the test section was covered with a thin film of current-conducting paint and a circuit established between it and the Pitot-tube, thereby causing a light to flash in the cockpit when the tube was in contact with the surface. The instrument could thus be zeroed in flight, thereby eliminating any zero errors resulting from changes in total head on the face of the instrument. The velocity in the boundary layer was read on a calibrated Kollsman helicopter airspeed indicator. Typical boundary layer mean velocity profiles obtained by the traversing mechanism are shown in Figure 11. Pressure distributions were obtained by means of 18 flush static pressure taps at suitable chordwise stations along the test section, connected to the multichannel photomanometer shown in Figure 10.

The experimental configurations tested besides the impervious case were suction and injection at slot angles of 1^{o}, 45^{o}, 90^{o}, 135^{o}, and 179^{o} (as illustrated in Figure 12). All the flight tests were performed at a freestream velocity of 49.0 miles per hour.

The coordinate system was selected with S measured along the surface of the test section (figure 13), $S = 0$ being taken at an arbitrary position behind the stagnation point, and $s = S$ near the rear-wardmost position of the section.

All boundary layer parameters utilized were obtained directly from the experimental velocity profiles. In order to obtain the skin friction, both the law of the wall,

$$\frac{u}{U_\tau} = 5.6 + 5.6 \log \frac{y U_\tau}{\nu},$$

and the empirical equation due to Ludweig and Tillman (Reference 5),

$$\left(\frac{U_\tau}{U}\right)^2 = 0.123 \left(\frac{U_\theta}{\nu}\right)^{-.268} 10^{-.678H},$$

were employed and were found to give consistent results as shown in Figure 14. In each case, the value of U_τ finally selected was a mean between the results predicted by each method.

The flight tests were carried out at pressure altitudes ranging between sea level and 10,000 feet using an altimeter setting of 29.92. The problem of varying Reynolds number could not, of course, be controlled to any extent due to the constantly decreasing altitude of the sailplane and the variations in the lapse rate. Fortunately, however, although a careful record of static air temperature and pressure was maintained throughout the tests, it was found that the maximum variation in Reynolds number was less than 10 percent. The average deviation from a given mean value was very much less than this, and therefore no significance was attached to this effect in analyzing the experimental data. Each Pitot-static airspeed system was dynamically balanced to account for the constantly changing static pressure resulting from the glide path of the sailplane.

To alter the transpiration angle, it was necessary to change the slotted plate in the test section; and this procedure, since it involved complete refinishing and periodic modification of the section, invariably resulted in a sufficient alteration of airfoil geometry to affect the potential flow (Figure 15). In view of this, no attempt was made

to compare the results of the various configurations directly, and each case was dealt with individually.

DISCUSSION OF RESULTS

The experimental results have indicated that the flow immediately downstream of the slot remains attached for moderate injection quantities, and that the transpiration does not substantially affect the local potential velocity (Figure 16). The assumption that the entire effect of the transpiration takes place over the slot width is not physically plausible; and in reality, entrainment processes cause the effects of transpiration to be felt both upstream and downstream of the slot, thereby avoiding an abrupt change in the boundary layer in the neighborhood of the slot. This effect is illustrated in Figure 17, where the momentum loss thickness 25 slot widths upstream of the slot is seen to be a definite function of the quantity flow through the slot but exhibits no discernable dependence on the slot angle, σ . The simplification permitted by this assumption in the design of an appropriate theoretical model justifies its existence provided that the actual physical picture is kept in mind. The plausibility and necessity of assuming a linear change in shearing stress over the slot are justified since the viscous forces acting upon the control volume result from a complex interaction between the slot and boundary layer flows, so that any attempt to delve into the detailed mechanics of the problem would constitute a major undertaking in itself. Fortunately, it turns out that the terms involving the shearing forces are of a minor order and thus may be neglected in most cases. Presuming a linear change in potential velocity and shearing stress across the slot follows directly from the assumption that the quantity $\omega' = \frac{\omega}{\sin\sigma}$ is small with respect to the characteristic dimension of the body, so that any deviation from linearity over such a short distance would in practice be undetectable.

Figures 18, 19 and 20 demonstrate the ability of equation 9 to adequately predict the change in momentum loss thickness across the slot. It is noted that the experimental points do not display a discontinuity but form continuous curves in the vicinity of the slot, which was, of course, anticipated. It is also noted from these figures that the growth of θ behind the slot follows an almost identical pattern regardless of whether the boundary layer has been energized, inflected, or unaffected by the transpiration. This evidence substantiates the assumption that the momentum loss thickness development downstream of a transpiration slot is a function only of the initial value of θ and the velocity distribution over the surface. The method of Von Doenhoff and Tetervin was selected on the basis of its simplicity and reliability and has given satisfactory results in the present analysis.

Once the value of θ was known at every downstream position, the corresponding values of U_2 were found from equation 10 and plotted in Figures 22, 23 and 24; and the agreement between the theoretical predictions and the experimental data is seen to be satisfactory.

Figure 21 indicates that the theory predicts values of θ which are low in cases where separation and reattachment occur behind the slot. This is due to the fact that the jet of air issuing from the slot serves to separate the boundary layer and to act as a vortex generator, stimulating turbulent entrainment of energy from the free stream and thereby providing sufficient energy to accomplish the reattachment even in the adverse pressure gradient existing in the neighborhood of the slot. A net momentum loss is suffered; consequently, the value of θ of the reattaching boundary layer is higher than expected by the theory.

It is intuitively expected that injection at some angle opposite to the direction of flow would be most effective in reducing the local skin friction. It has been found that this is indeed the case, but this reduction in the local skin friction is accompanied by a maximum increase in the momentum loss thickness. This optimum angle for reducing skin friction is, however, between $\frac{\pi}{2}$ and π and is a function of v_0 and v_{τ_1}. Figures 22, 23 and 24 illustrate the fact that only a small reduction in turbulent skin friction results from the slot injection, and this decrement is not well preserved downstream. In order to achieve a substantial decrease in the surface shearing stress, the injection velocity must be of a sufficient magnitude to separate the boundary layer locally. The assumed form of this decrease in v_τ to the point of separation is sketched in the figures. This entails substantial energy losses with a consequential large wake buildup, and even then the decrease in skin friction endures only a very short distance downstream of the slot.

Equations 8 and 9 and Figure 2 indicate that the overall effect of the angle σ upon the change in momentum loss thickness is small, particularly at low or moderate slot quantity flows, and the magnitude of the transpiration quantity is the predominant factor in the analysis.

The theoretical analysis for suction slots may be extended directly to laminar flow, provided that the Reynolds number, slot shape, and slot velocity are such that they do not promote transition to turbulence. The calculation procedure is unchanged except that the methods used for calculating the development of θ on an impervious surface is replaced by the corresponding laminar technique. The methods described by Schlichting (Reference 6) provide a rapid and accurate means by which these quantities may be obtained in an arbitrary pressure gradient.

It must be observed that if σ is close to 0 or π, the theoretical analysis tends to weaken somewhat, since $\omega' = \frac{\omega}{\sin\sigma}$ becomes large and the assumption that this term is small with respect to the characteristic length of the body under consideration may no longer be considered reasonable. As a result of this, the other assumptions also begin to deteriorate; for example, if a substantial arbitrary pressure gradient exists over this type of slot, it may no longer be possible to presume a

linear drop in potential velocity across the slot, not to mention neglecting the change entirely. In addition, more precise information would be required concerning the forces generated at the free boundary of the control volume due to the interaction between the slot and boundary layer flows. The above-mentioned complications do not enter the problem to a significant degree until the angle made between the axis of the slot and the surface is less than about 10°. Thus, for most practical cases, the theory is applicable. The boundary layer in the vicinity of the extreme angled slots $\sigma = 1^{\circ}$ and $\sigma = 179^{\circ}$, while not strictly subject to the mathematical treatment of the Theoretical Considerations section, did behave in the general manner indicated by the theory. For example, injection at $\sigma = 1^{\circ}$ does not appreciably effect the boundary layer, while injection at $\sigma = 179^{\circ}$ causes a substantial increase in momentum loss thickness as shown in Figure 25. In similar fashion, Figure 26 indicates that suction at $\sigma = 1^{\circ}$ is more effective in decreasing θ than suction at $\sigma = 179^{\circ}$, although the quantity flow through the slot is in both cases the predominant factor. Figure 27 shown that the skin friction immediately downstream of the $\sigma = 179^{\circ}$ injection slot is appreciably reduced, but that this decrement is not well preserved downstream, even when the injection velocity is of a sufficient magnitude to effect local separation. This is in agreement with the results obtained with the moderate angled slots. It is suggested that the theoretical model of Figure 1 deteriorates to that shown in Figure 28 when the slot angle assumes extreme values (for example, $\sigma < 10^{\circ}$ or $\sigma > 170^{\circ}$); that is, a tangential slot with a corresponding alteration in surface geometry.

CONCLUDING REMARKS

The experimental data indicates that equations 8 and 9 are capable of predicting the effect of transpiration through angled slots on the development of the momentum loss thickness of a turbulent boundary layer. The theory fails, however, when the injection is of a sufficient magnitude to separate the boundary layer at the downstream edge of the slot. Additional research is required to investigate the behavior of the wall shearing stress at the downstream edge of the slot for very large suction quantities; for example, an approximate empirical expression relating U_{τ_2}, β_s and σ would enable equation 8 to describe this asymptotic condition. It has been observed that the subsequent development of the momentum loss thickness downstream of the slot is dictated by the initial value of θ behind the slot and the velocity distribution over the surface aft of the slot and in this respect is independent of the transpiration. The momentum integral equation may be employed to obtain values of the skin friction velocity U_τ at desired points behind the slot once the development of θ has been computed. The investigation has disclosed that the turbulent shearing stress is relatively insensitive to slot injection and that any local decrease is recovered for the most part a short distance downstream, only a small decrement in U_τ being preserved. This is true even when local separation occurs behind the slot, since reattachment follows almost immediately. The most effective angle for decreasing θ has been found to lie between 0 and $\frac{\pi}{2}$; however, this may not be the most efficient angle from the standpoint of blower power required since other factors such as the condition of the flow in the slot itself enter into the picture. Finally, at low or moderate slot velocities the influence of slot angle is small, as shown in Figure 2, and for most applications would, therefore, probably be dictated primarily by structural considerations.

REFERENCES

1. Williams, John, A Brief History of British Research on Boundary Layer Control for High Lift: Boundary Layer and Flow Control, G. V. Lachmann, Pergamon Press, New York, 1961.

2. McCullough, G. B., and Bault, D. E., An Experimental Investigation of the NACA 63-012 Airfoil Section with Leading Edge and Midchord Suction Slots, NACA TN 2041, February, 1950.

3. Roberts, Sean C., Unpublished Doctoral Thesis, University of London.

4. Von Doenhoff, A. E., and Tetervin, N., Determination of the General Relations for the Behavior of Turbulent Boundary Layers, NACA Report 772, 1943.

5. Ludweig, H., and Tillman, W., Investigations of the Wall-Shearing Stress in Turbulent Boundary Layers, NACA TM 1285, 1949.

6. Schlichting, H., Boundary Layer Theory, p. 251, McGraw-Hill Co., New York, 1960.

APPENDIX

Calculation of Turbulent Boundary Layers on Impervious Surfaces - The Method of Von Doenhoff and Tetervin

The momentum integral equation for a boundary layer on an impervious surface in an arbitrary pressure gradient may be written

$$\frac{d\theta}{ds} + (H+2)\frac{\theta}{U}\frac{dU}{ds} = \frac{\tau_0}{\rho U^2} = \frac{c_f}{2} . \tag{A-1}$$

Suppose the skin friction coefficient assumes the form

$$c_f = A\left(\frac{U\theta}{\nu}\right)^{-n} \tag{A-2}$$

where the coefficient A and the exponent n are selected to correspond with the desired range of Reynolds numbers. For any particular application, the two constants of equation A-2 may be found by making equation A-2 agree with the assumed skin friction law at two values of $R_\theta = \frac{U\theta}{\nu}$ including the range under consideration. If the subscript corresponds to conditions at the low value of R_θ and 2 to conditions at the high value of R_θ, then

$$n = \frac{\log \dfrac{(\tau_0/\rho U^2)}{(\tau_0/\rho U^2)_2}}{\log (R_{\theta_2}/R_{\theta_1})}$$

$$A = c_{f_1} R_{\theta_1}^{\,n} .$$

The assumed skin friction law given by Squire and Young is

$$\frac{\tau_0}{\rho U^2} = \left[5.89 \log (4.075 R_\theta)\right]^{-2} .$$

Thus n and A are evaluated.

Examination of equation A-1 indicates that the value of $(H+2)$ is not greatly affected by the value of H, and that if the equation were integrated, θ would be little affected by variations of H within the extremes of the turbulent range ($H=1.2$ and $H=2.6$). Thus with H assumed constant and equal to 1.5, equation A-1 is seen to be of the Bernoulli form and may be integrated to give the value of θ as follows:

$$\frac{\theta}{s} = \left(\frac{U}{U_\infty}\right)^{-3.5} \left[\frac{(1+n)A}{2\,\frac{U_\infty s}{\nu}} \int_{s_i/s}^{s/s} \left(\frac{U}{U_\infty}\right)^{3.5(n+1)+1} d\left(\frac{s}{s}\right) + \left(\frac{s_i}{s}\right)^{n+1} \left(\frac{U_{slot}}{U_\infty}\right)^{3.5(n+1)} \right]^{\frac{1}{1+n}}$$

This equation may be applied directly to calculate θ at any point downstream of the slot.

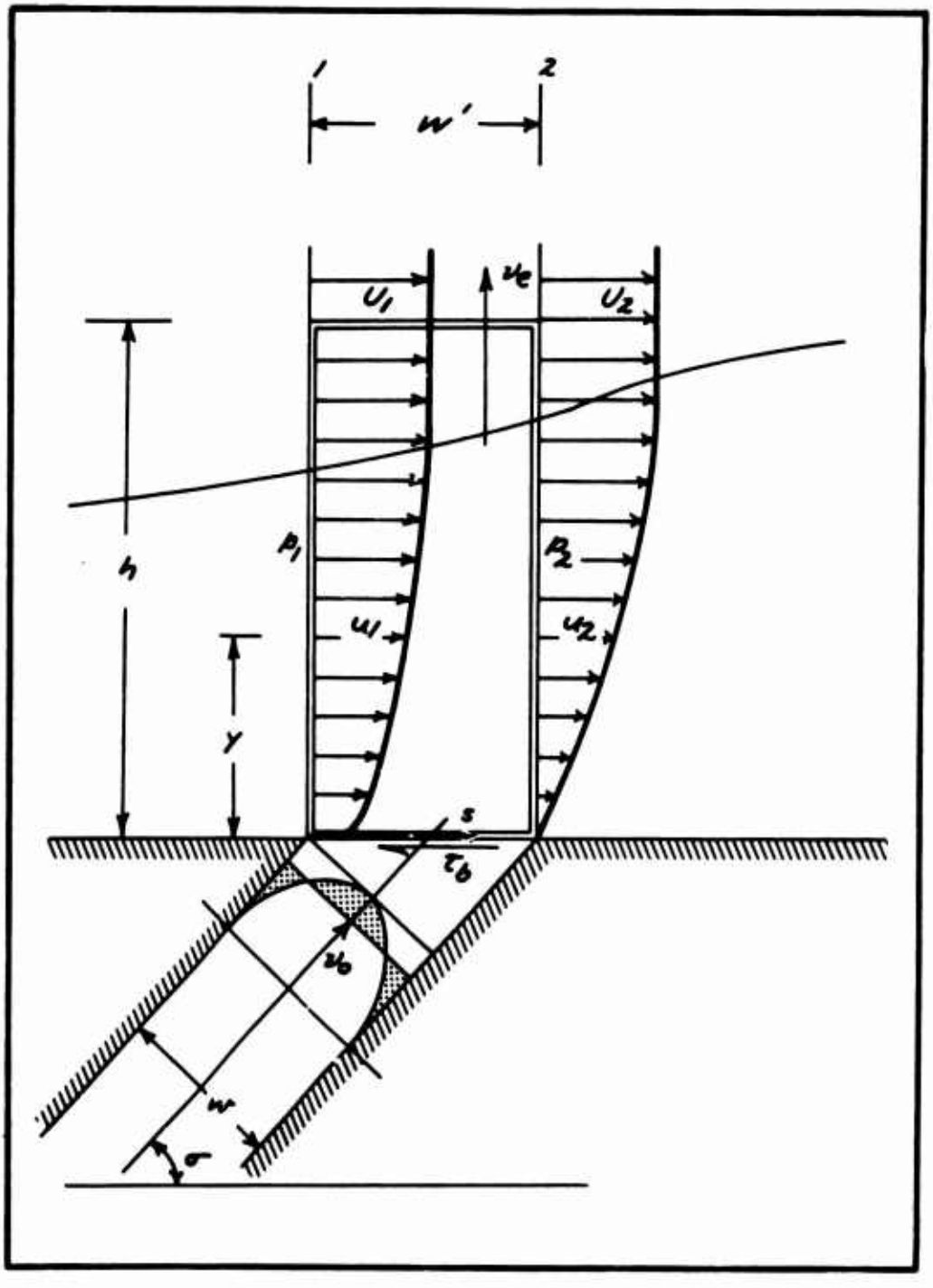

Figure 1. Theoretical Model of Conditions Existing at Angled Slot.

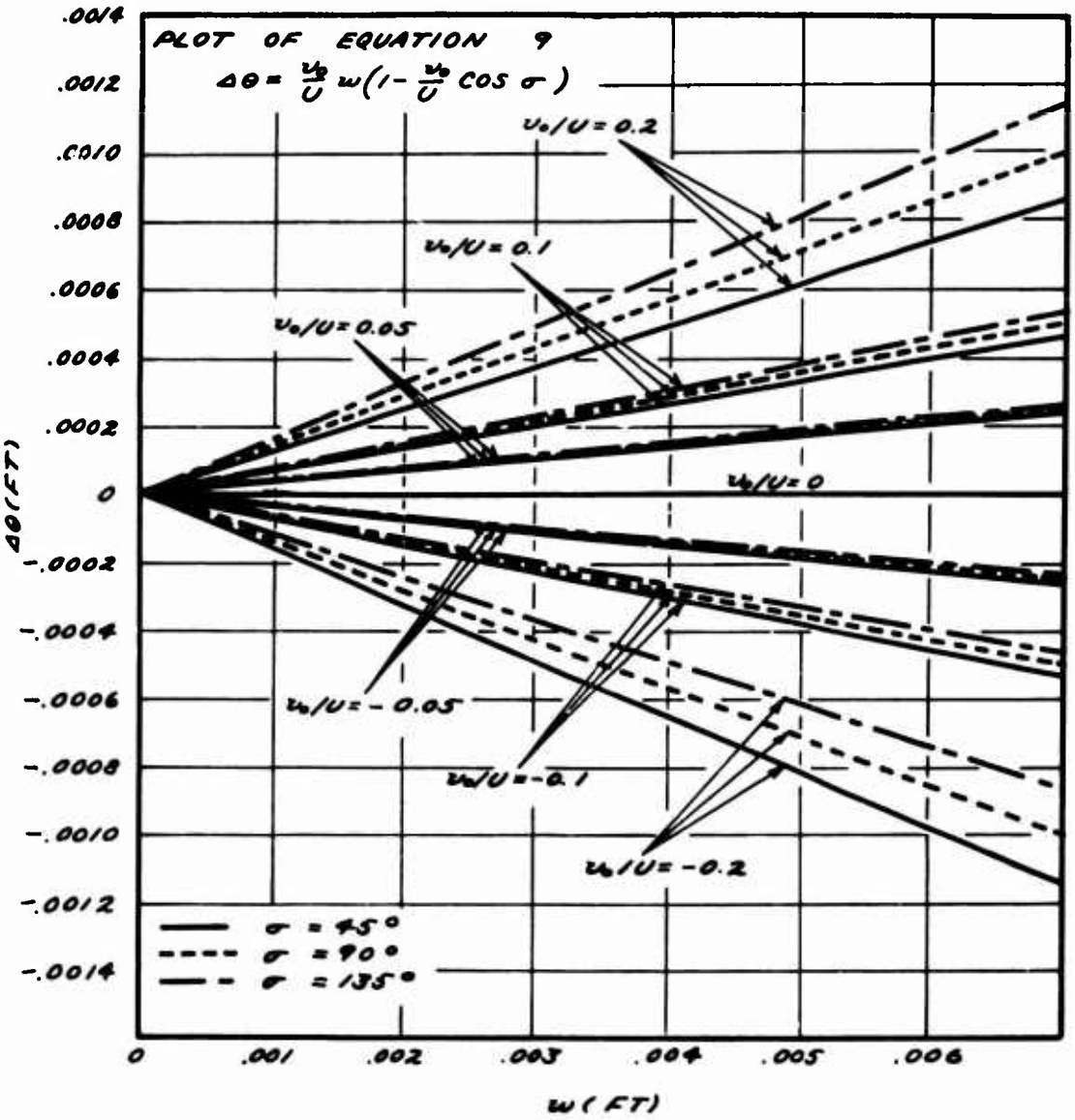

Figure 2. Influence of Slot Parameters Upon Change of Momentum Loss Thickness Across Angled Slot.

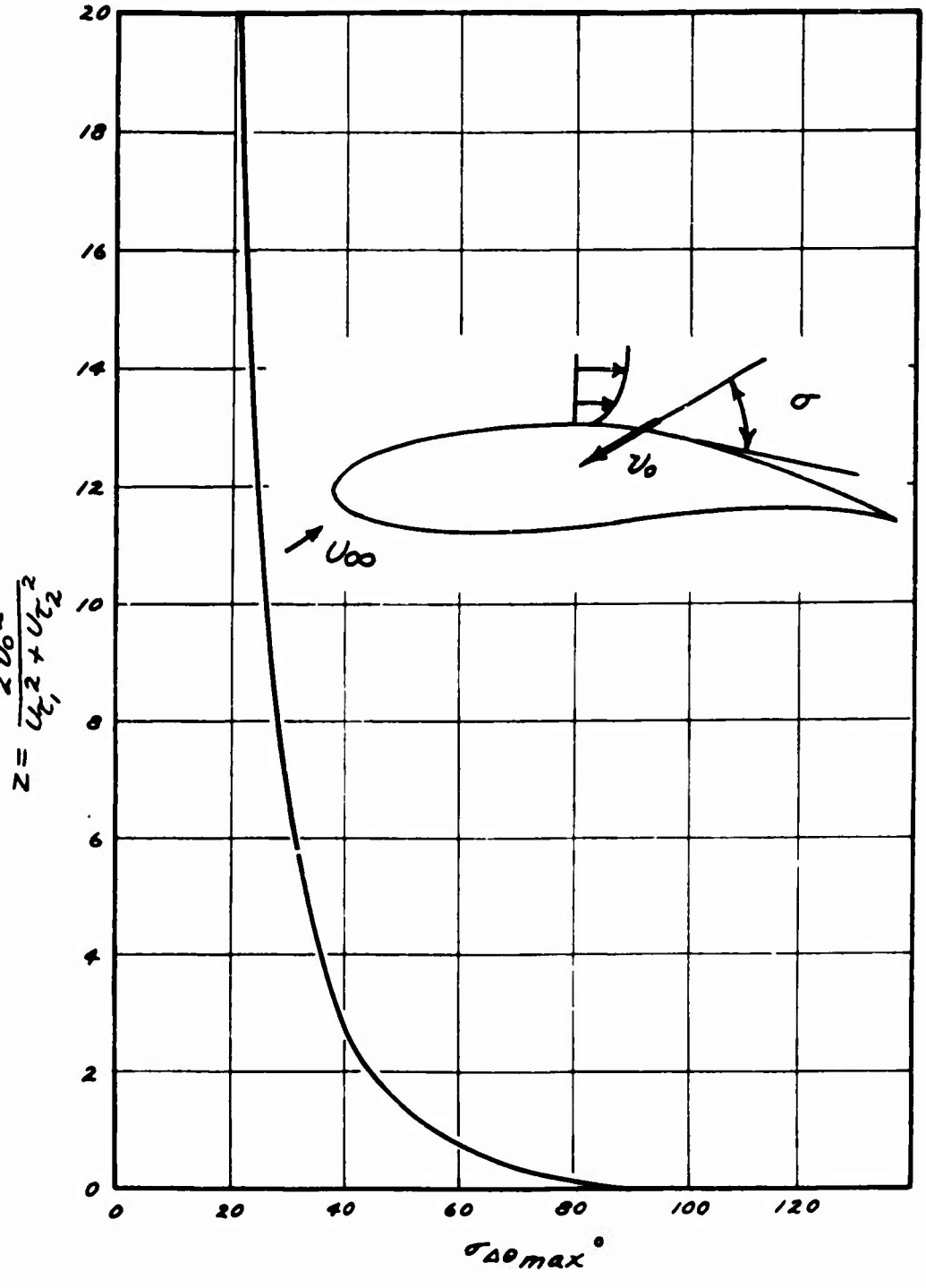

Figure 3. Most Effective Slot Angle to Change θ by Suction Against the Parameter Z Where $Z = \frac{2v_0^2}{U_{\tau_1}^2 + U_{\tau_2}^2}$.

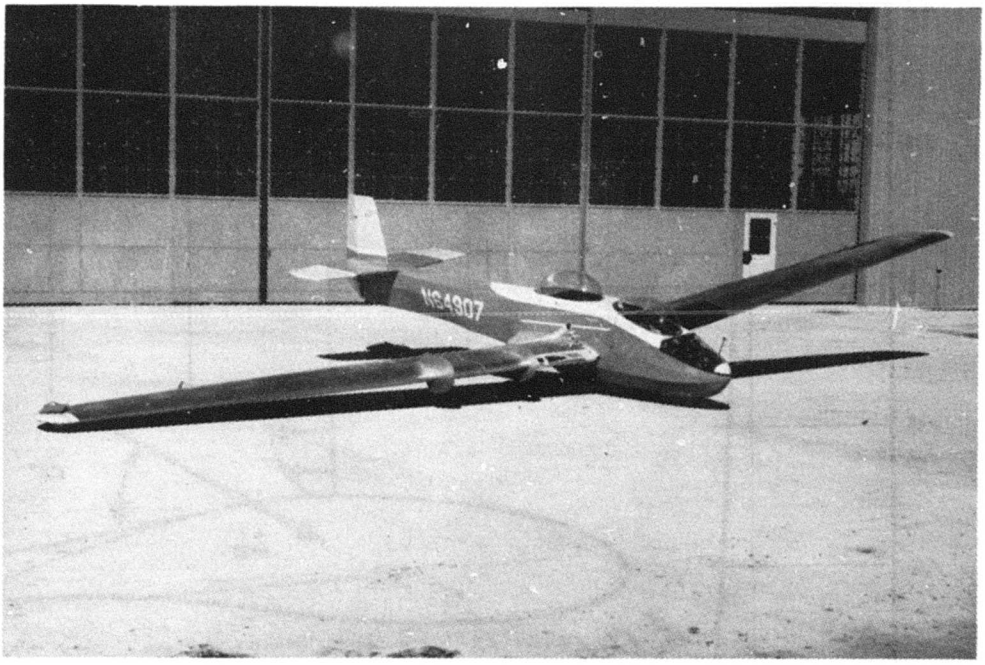

Figure 4. TG-3 Sailplane Used for the Flight Experiments.

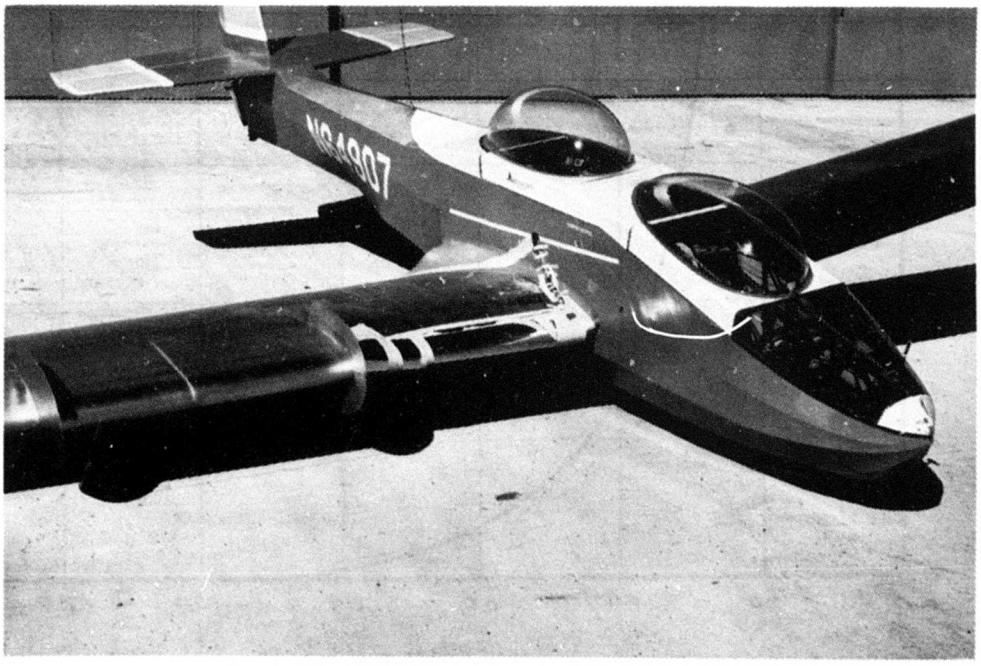

Figure 5. View of Test Section and Leading Edge Fairing.

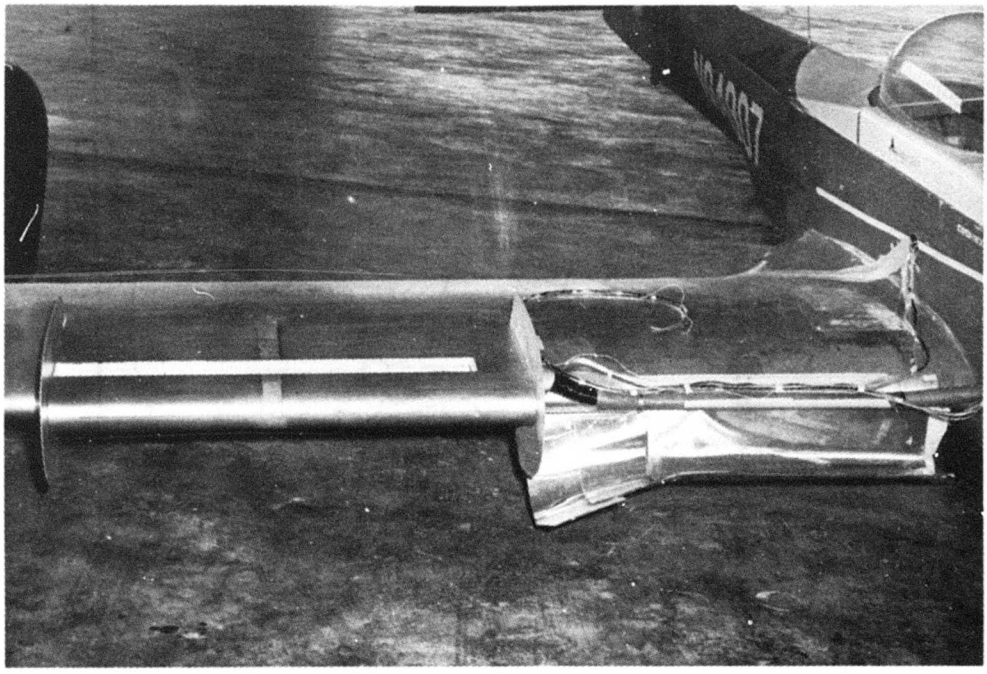

Figure 6. View of Slot Pressure Chamber and Ducting.

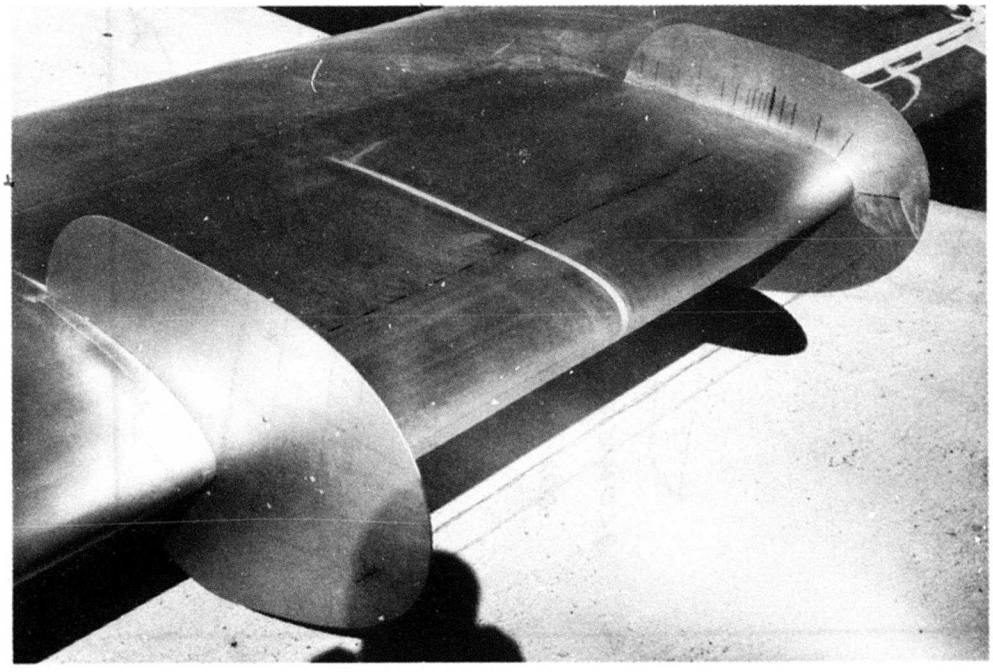

Figure 7. Detailed View of Test Section Showing the Slot, the Conducting Strip of Paint and the Wire Turbulence Generators.

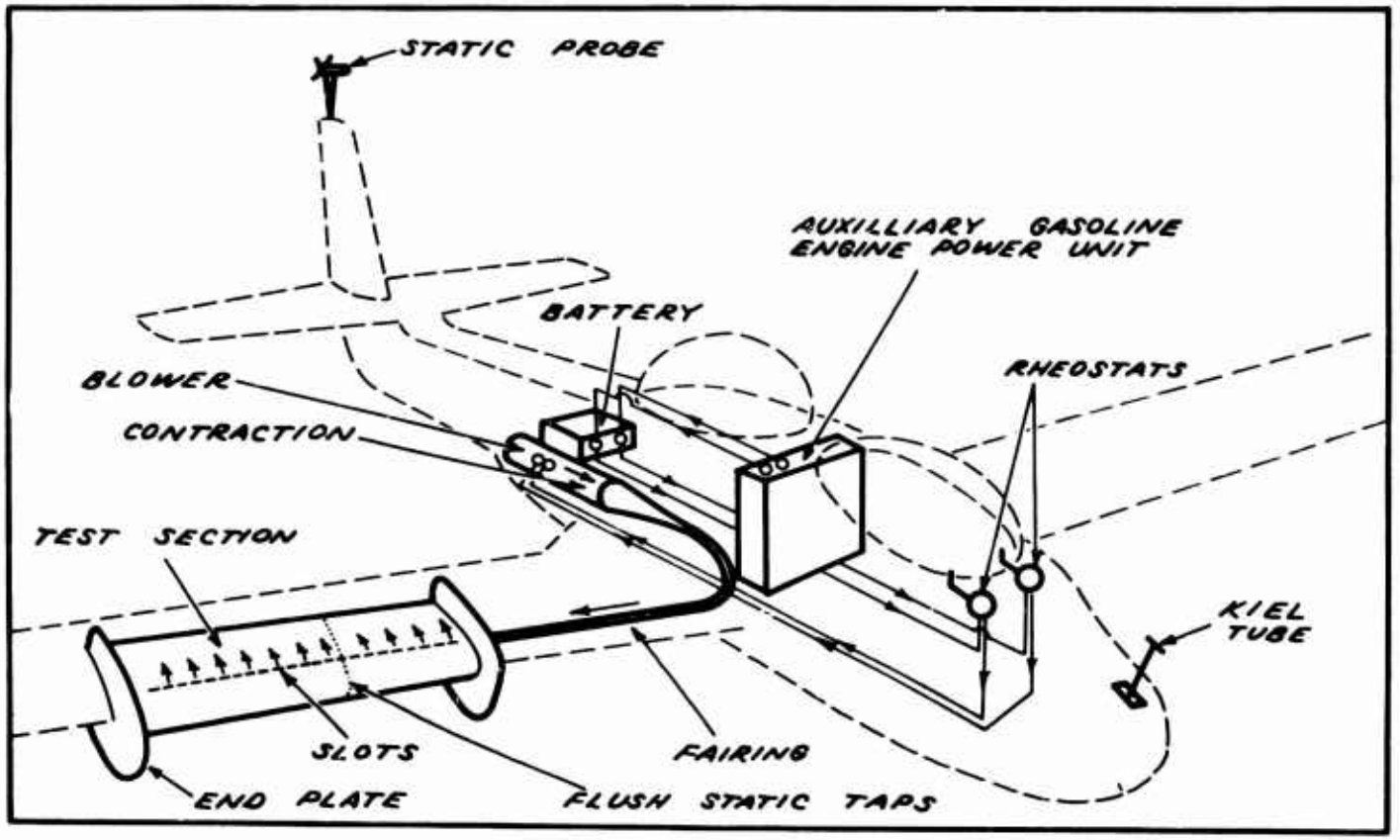

Figure 8. Schematic Diagram Showing General Arrangement of Experimental Apparatus.

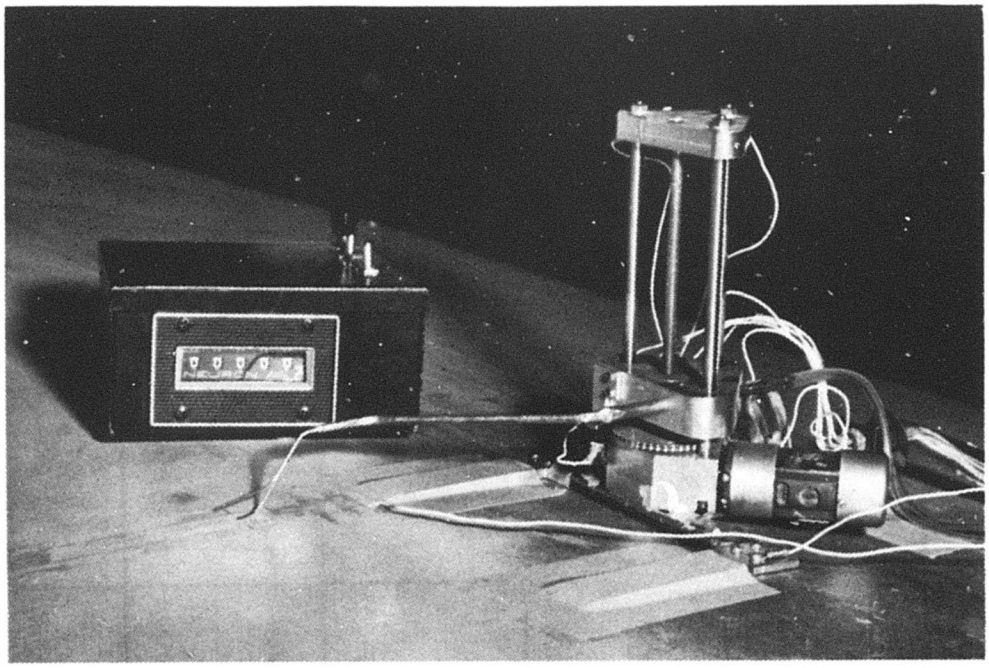

Figure 9. Boundary Layer Pitot-Static Traversing Mechanism.

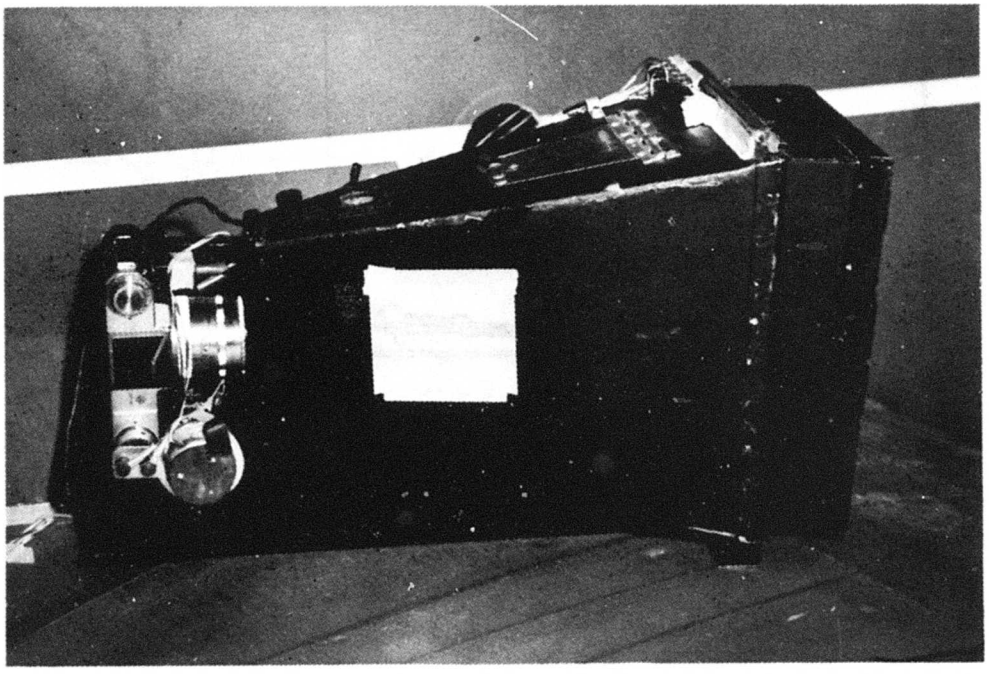

Figure 10. Multichannel Photomanometer.

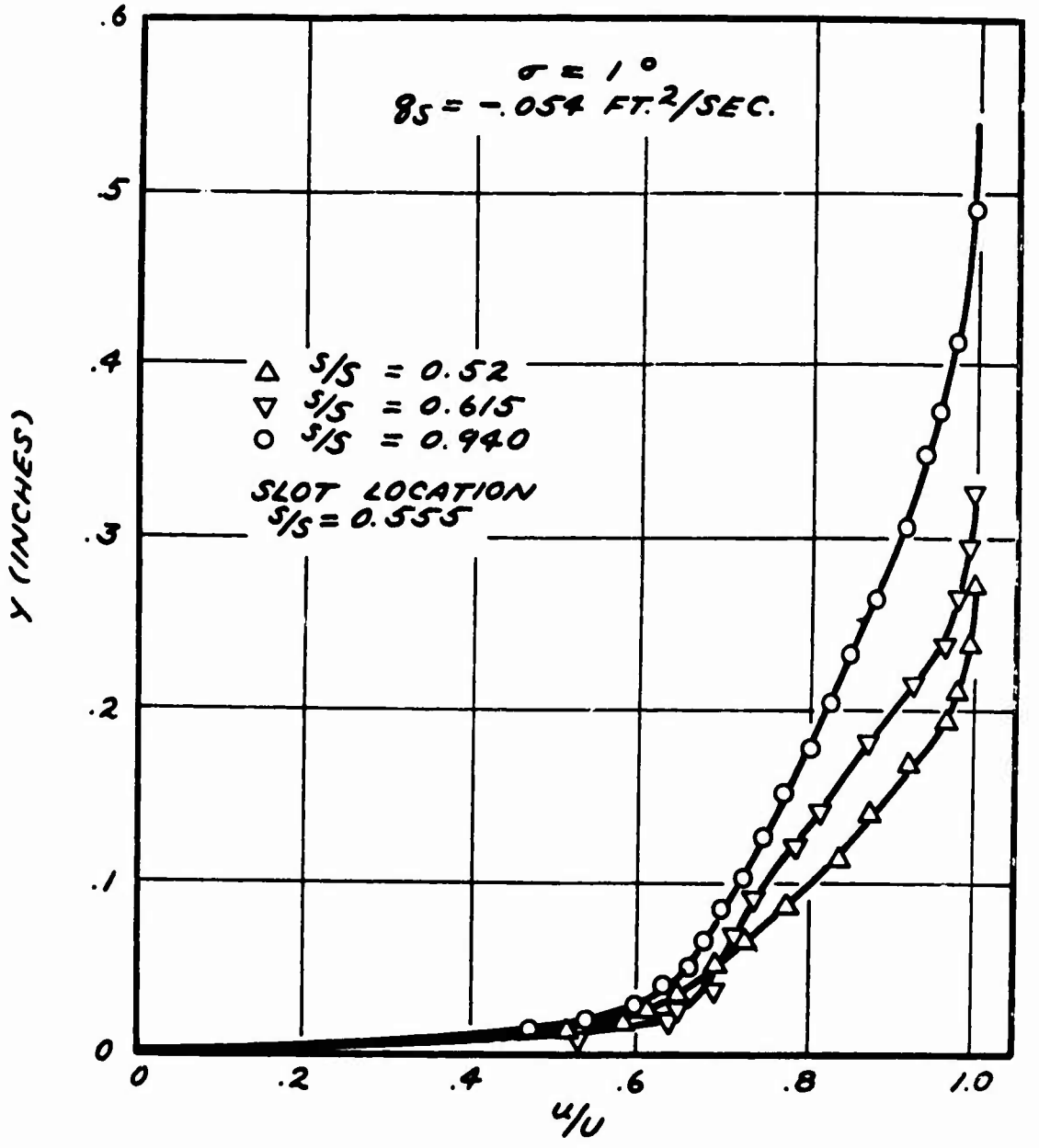

Figure 11. Typical Boundary Layer Velocity Profiles Obtained by Means of Pitot-Static Traversing Apparatus.

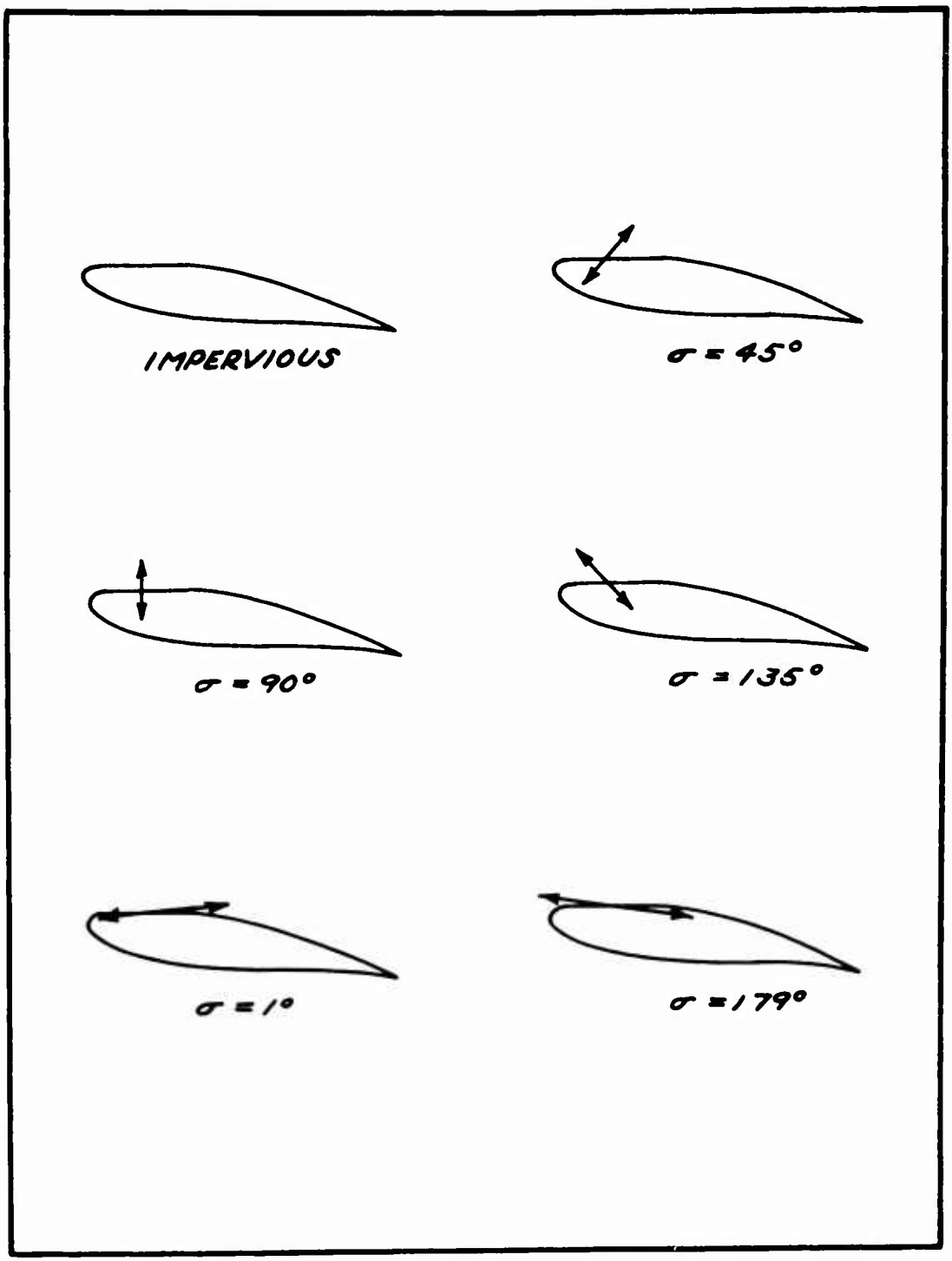

Figure 12. Experimental Configurations Investigated.

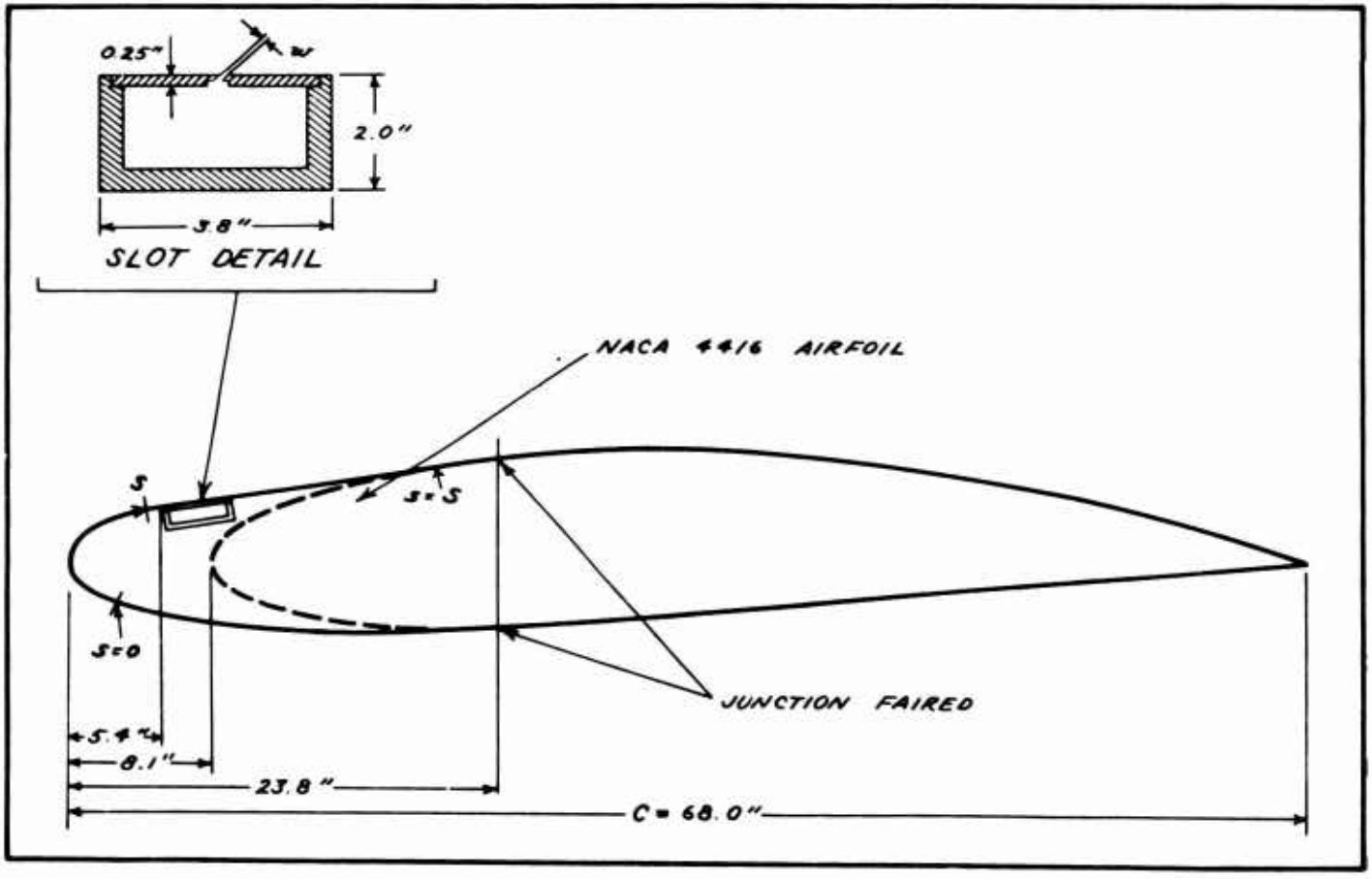

Figure 13. Geometry of Airfoil Test Section.

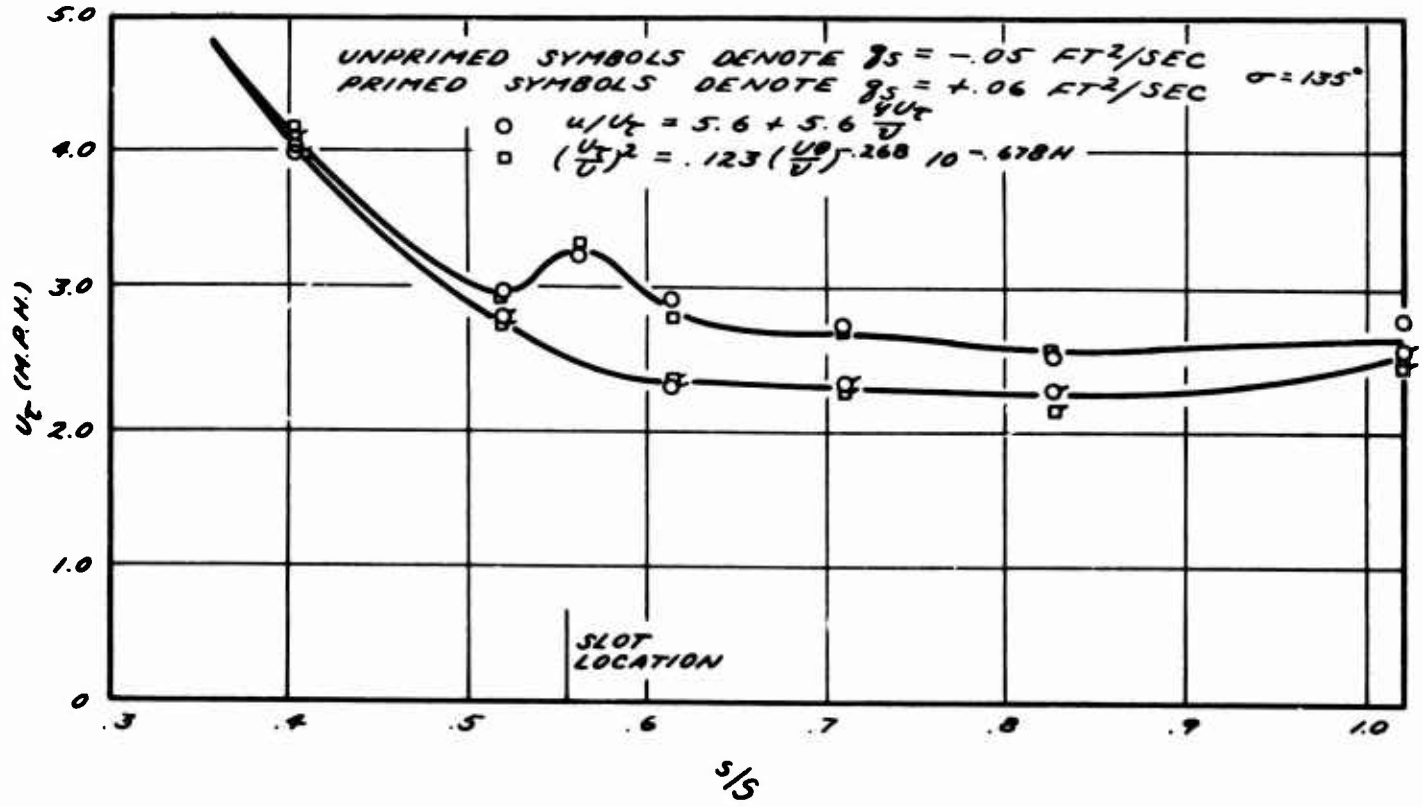

Figure 14. Comparison of Two Skin Friction Relationships for the Evaluation of U_τ from the Experimental Boundary Layer Profiles.

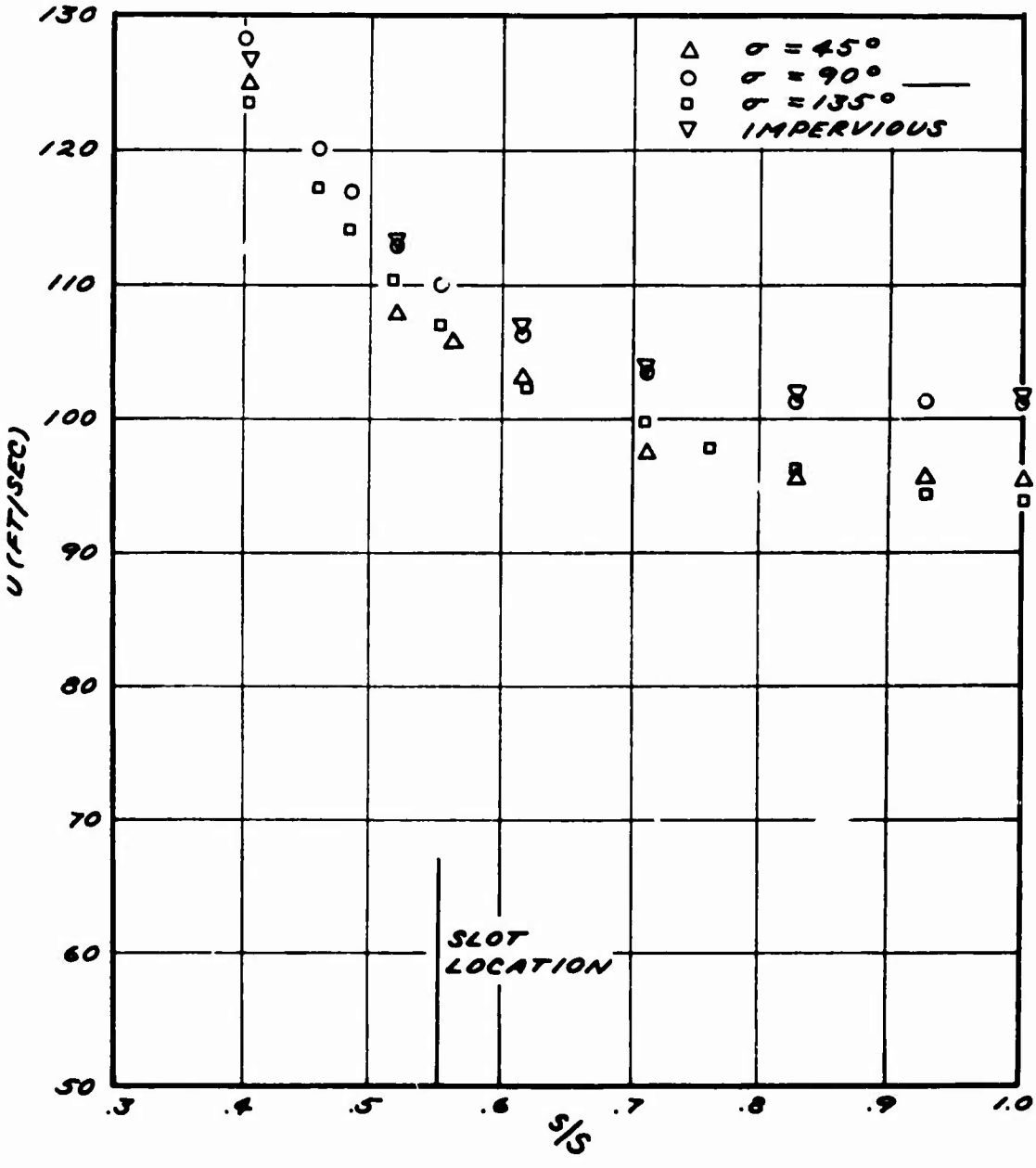

Figure 15. Velocity Distributions Over Test Section for Various Insert Plates, U_{∞} = 49.0 M.P.H.

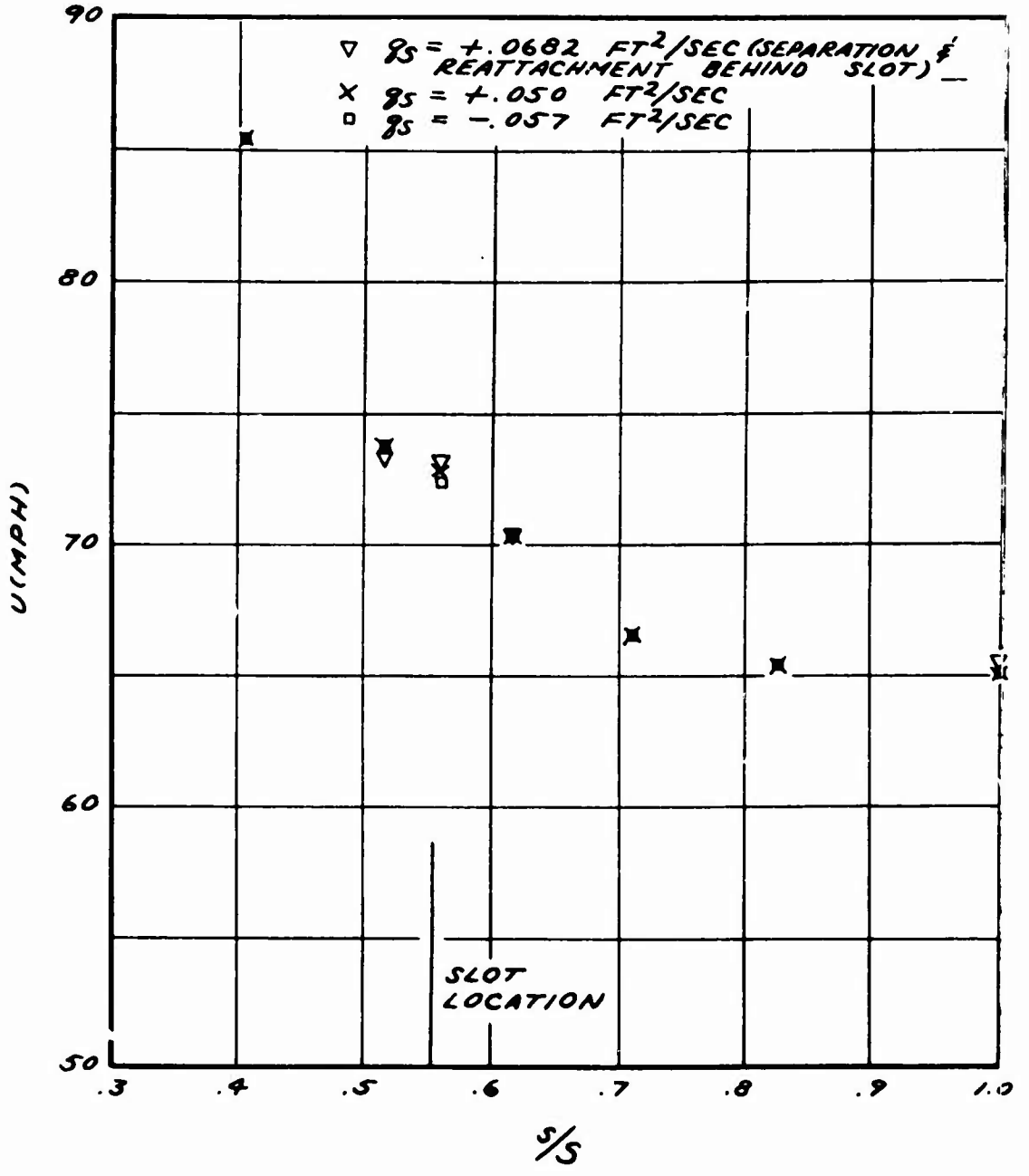

Figure 16. Effect of Transpiration on Velocity Distribution Over the Surface of the Test Section, 45° Slot.

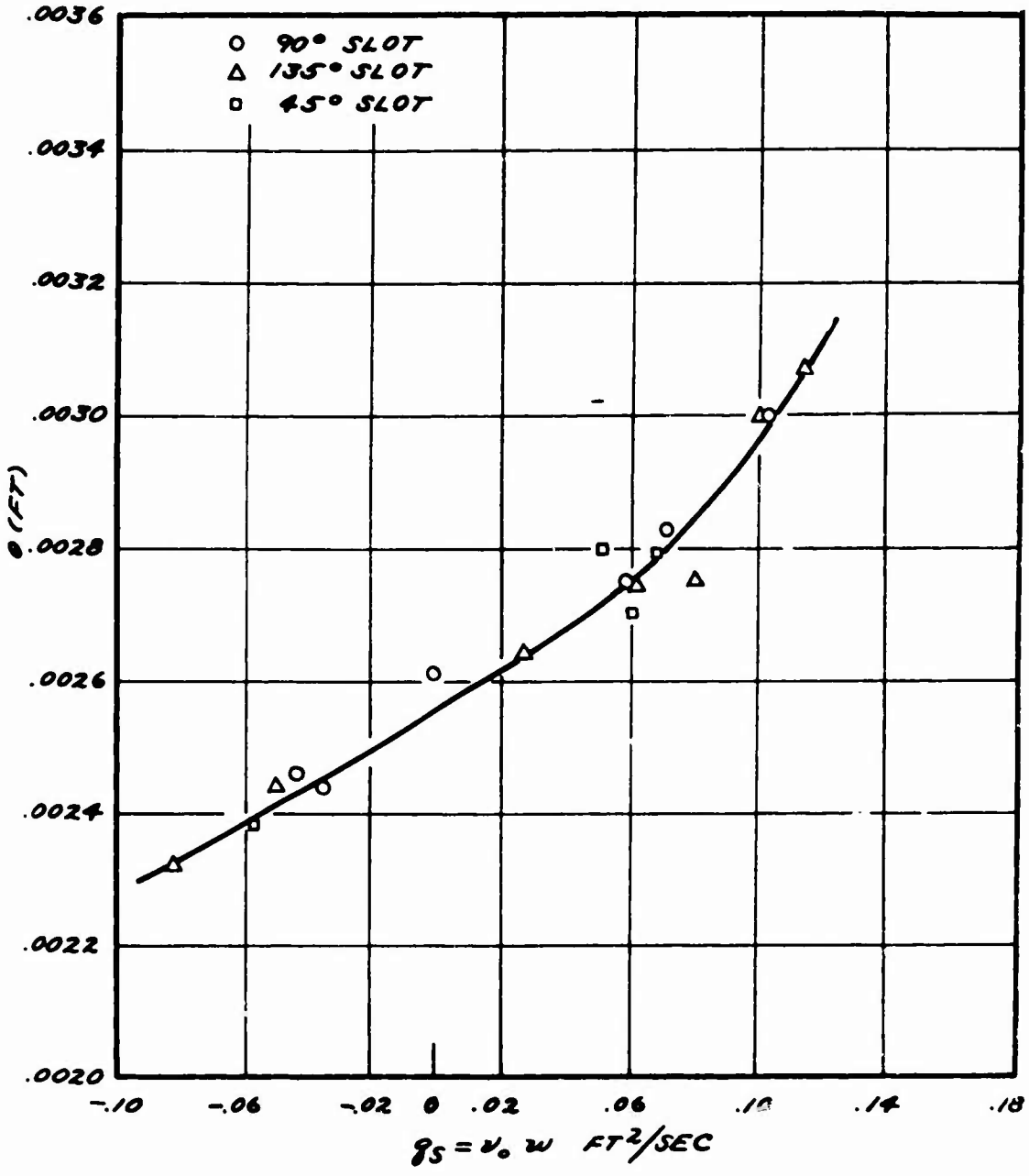

Figure 17. Influence of Slot Flow on the Momentum Loss Thickness Slot Widths Upstream of the Slot.

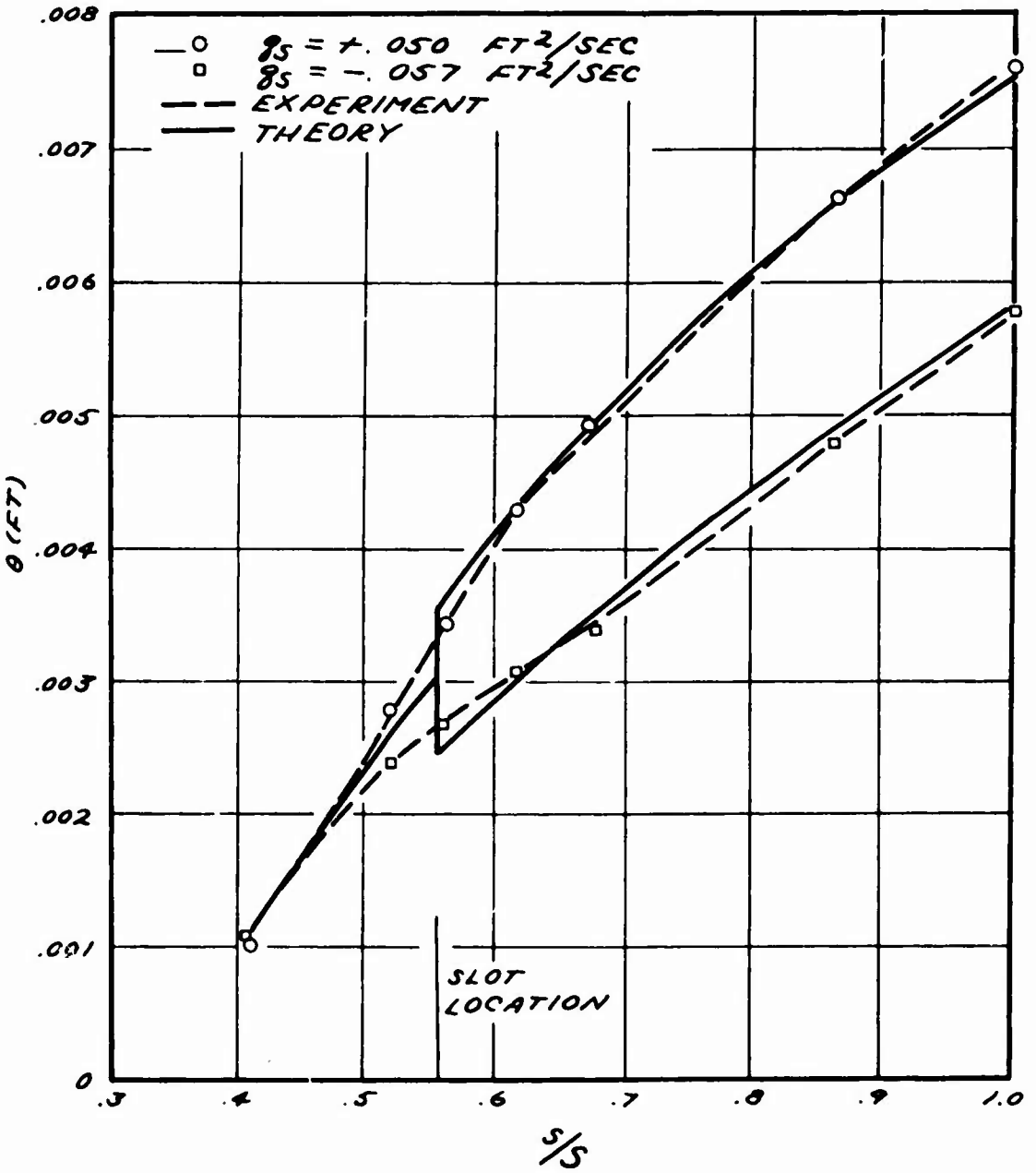

Figure 18. Effect of Transpiration on the Development of the Momentum Loss Thickness θ in Case of the 45° Slot.

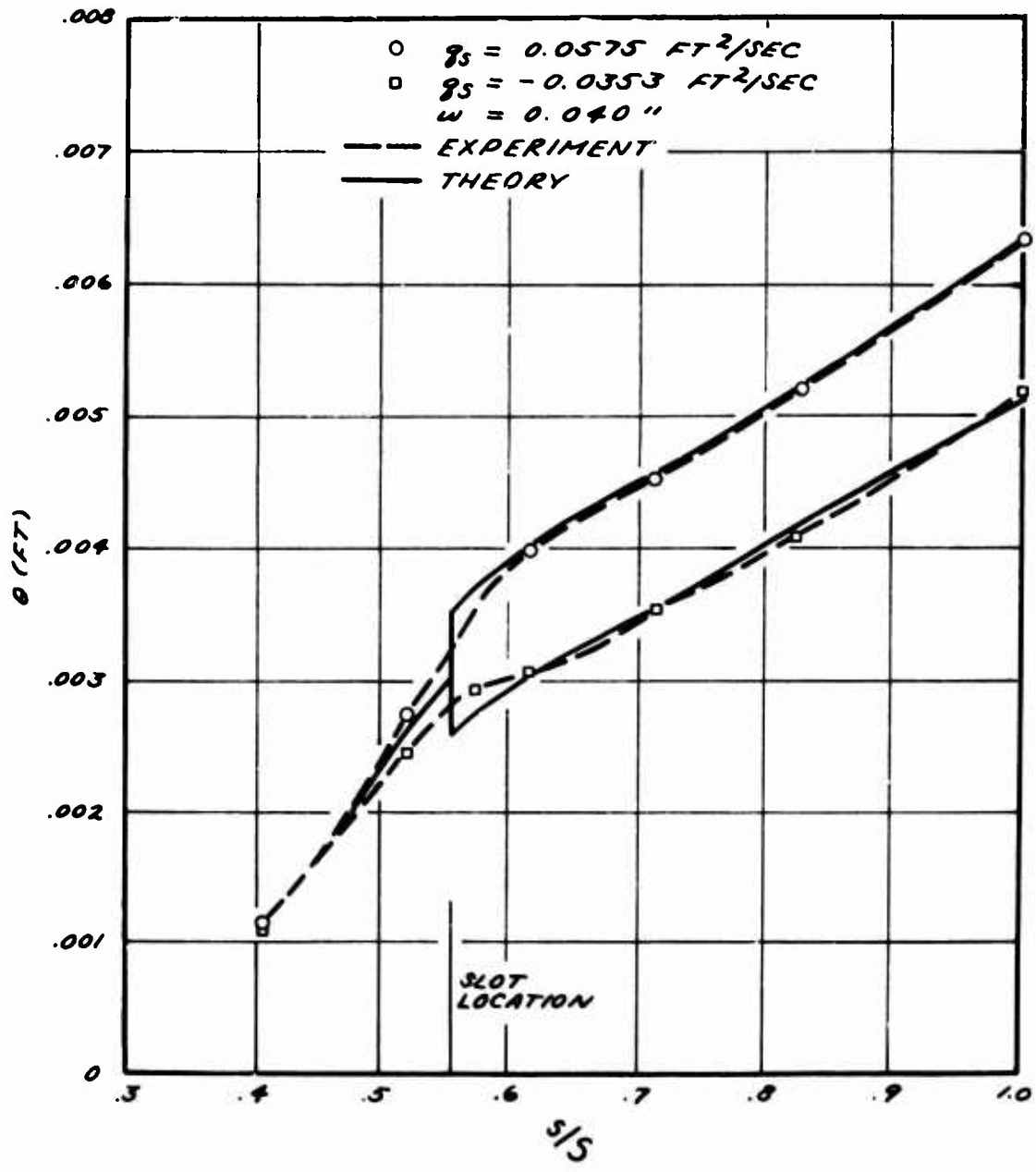

Figure 19. Development of Momentum Loss Thickness θ for Case of the 90° Slot.

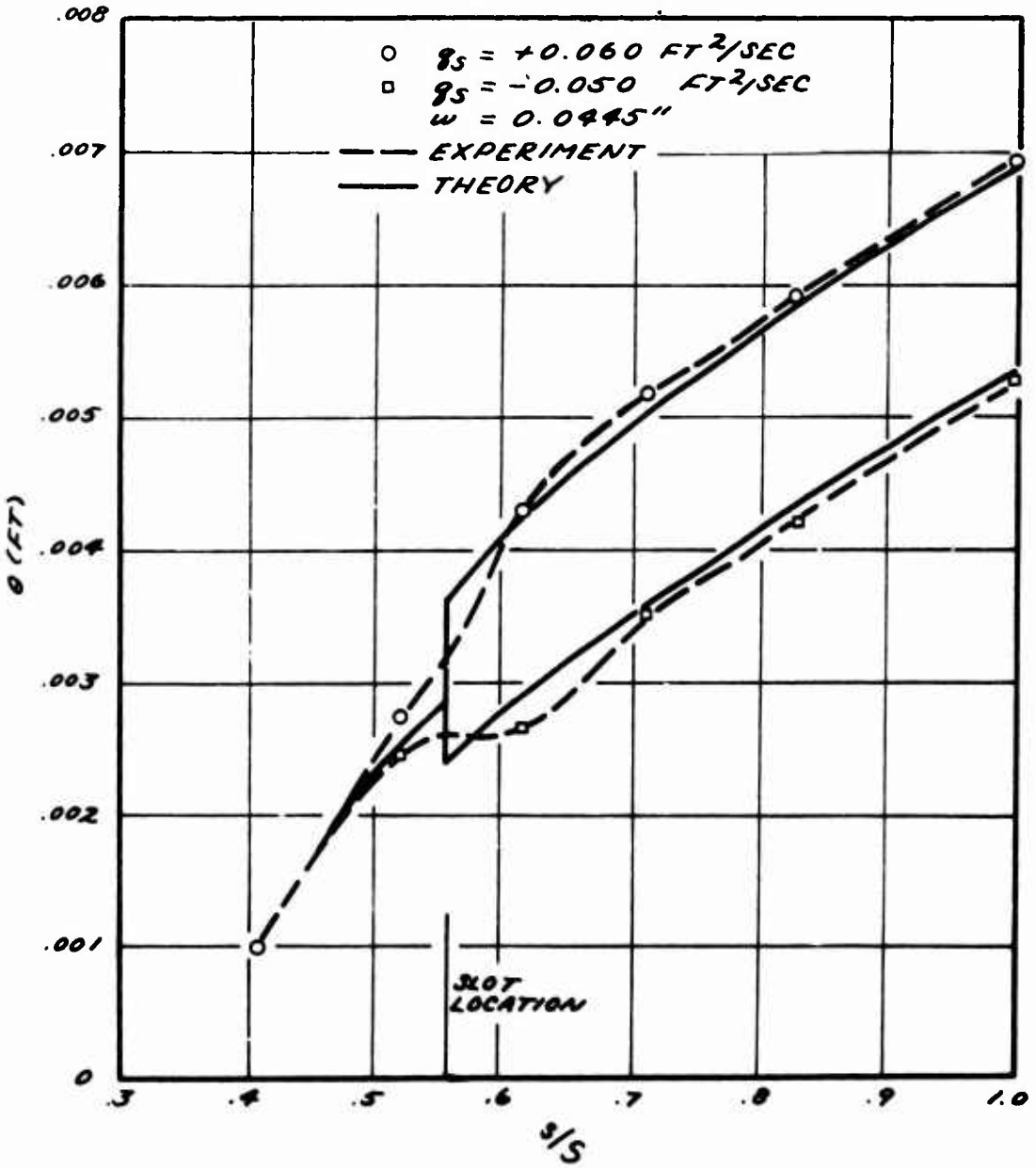

Figure 20. Development of Momentum Loss Thickness θ for Case of the 135° Slot.

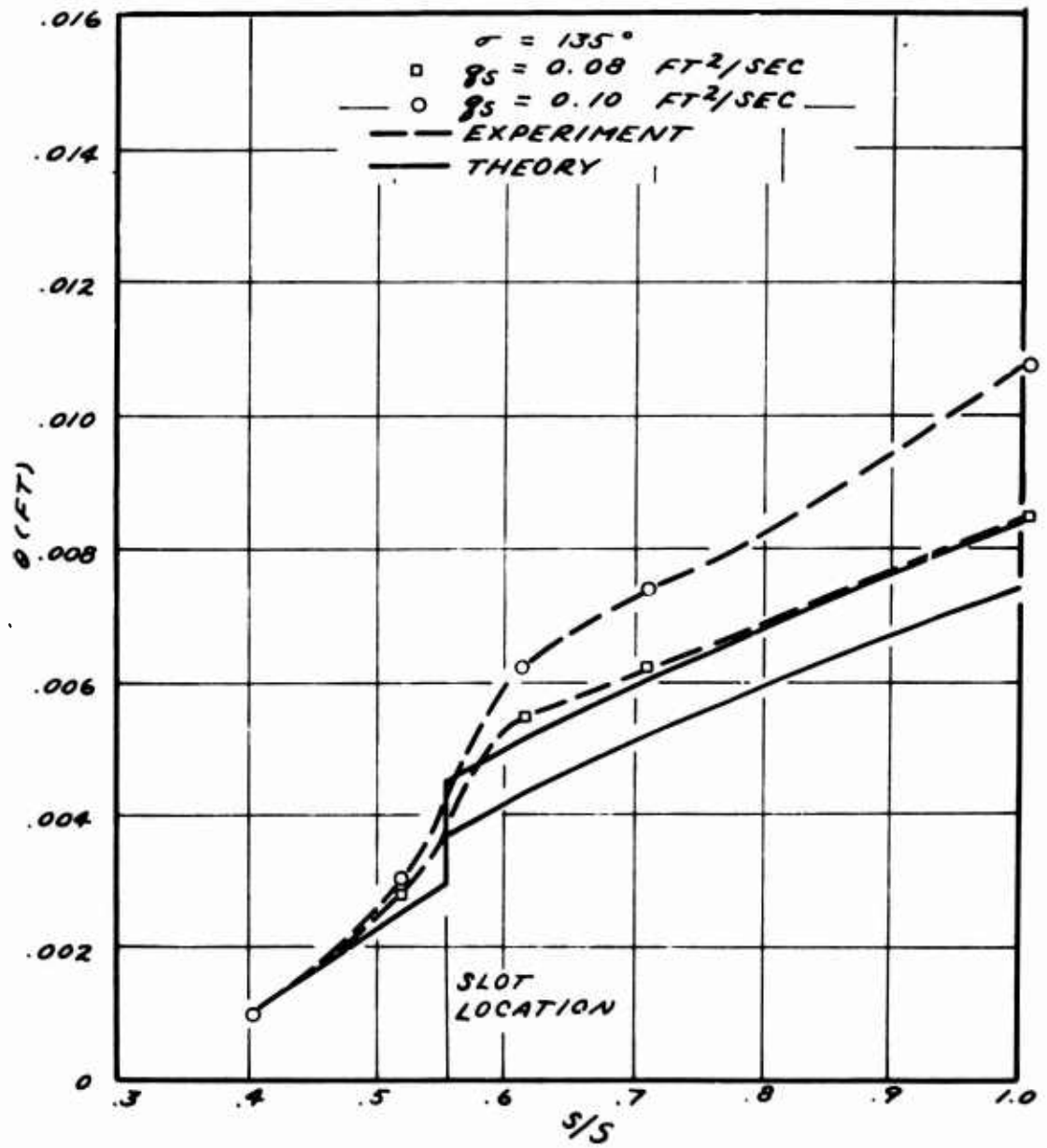

Figure 21. Failure of the Theory in Cases Where Separation and Reattachment Occur Downstream of the Slot.

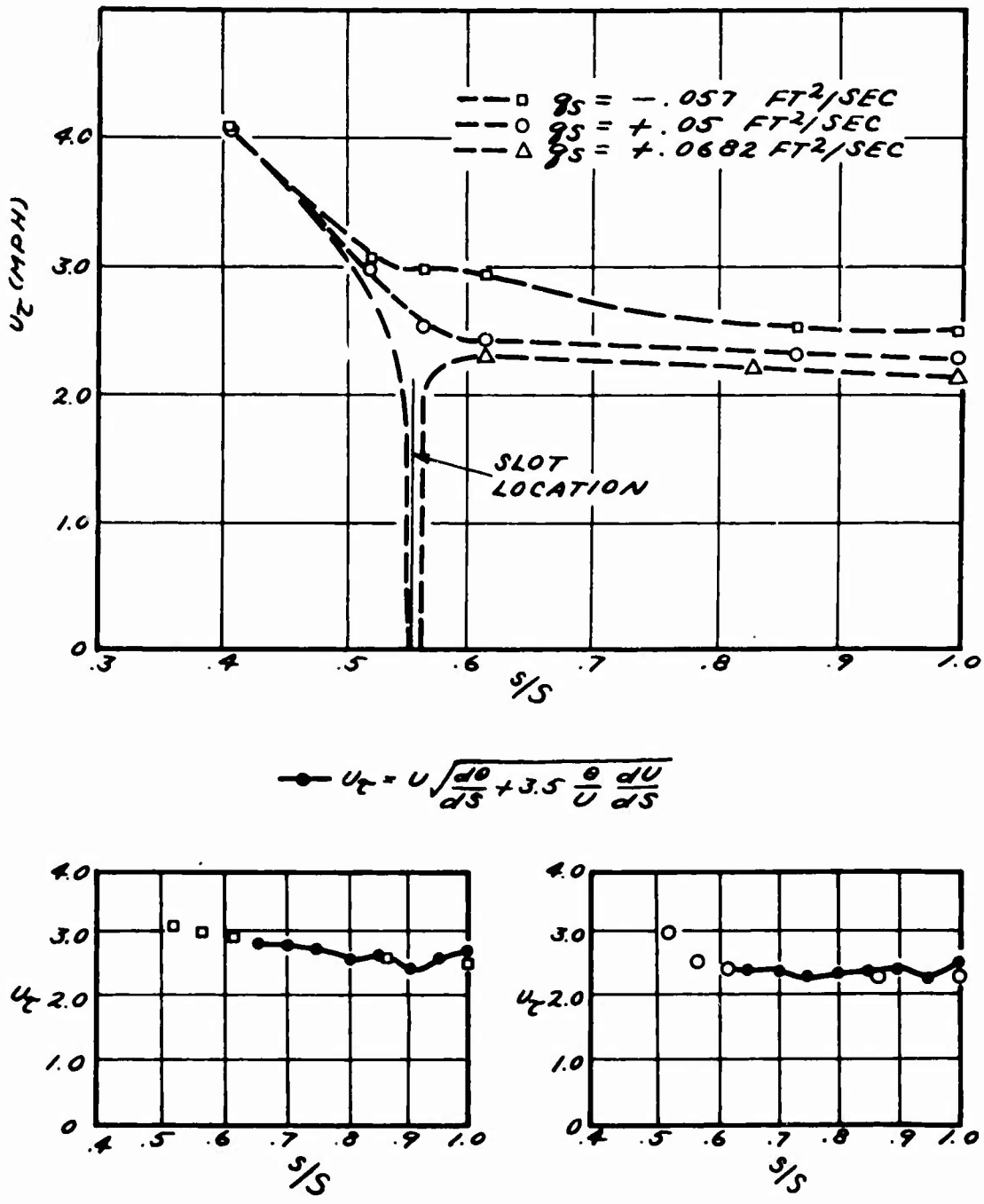

Figure 22. Effect of Transpiration on Friction Velocity U_τ in Case of the 45° Slot.

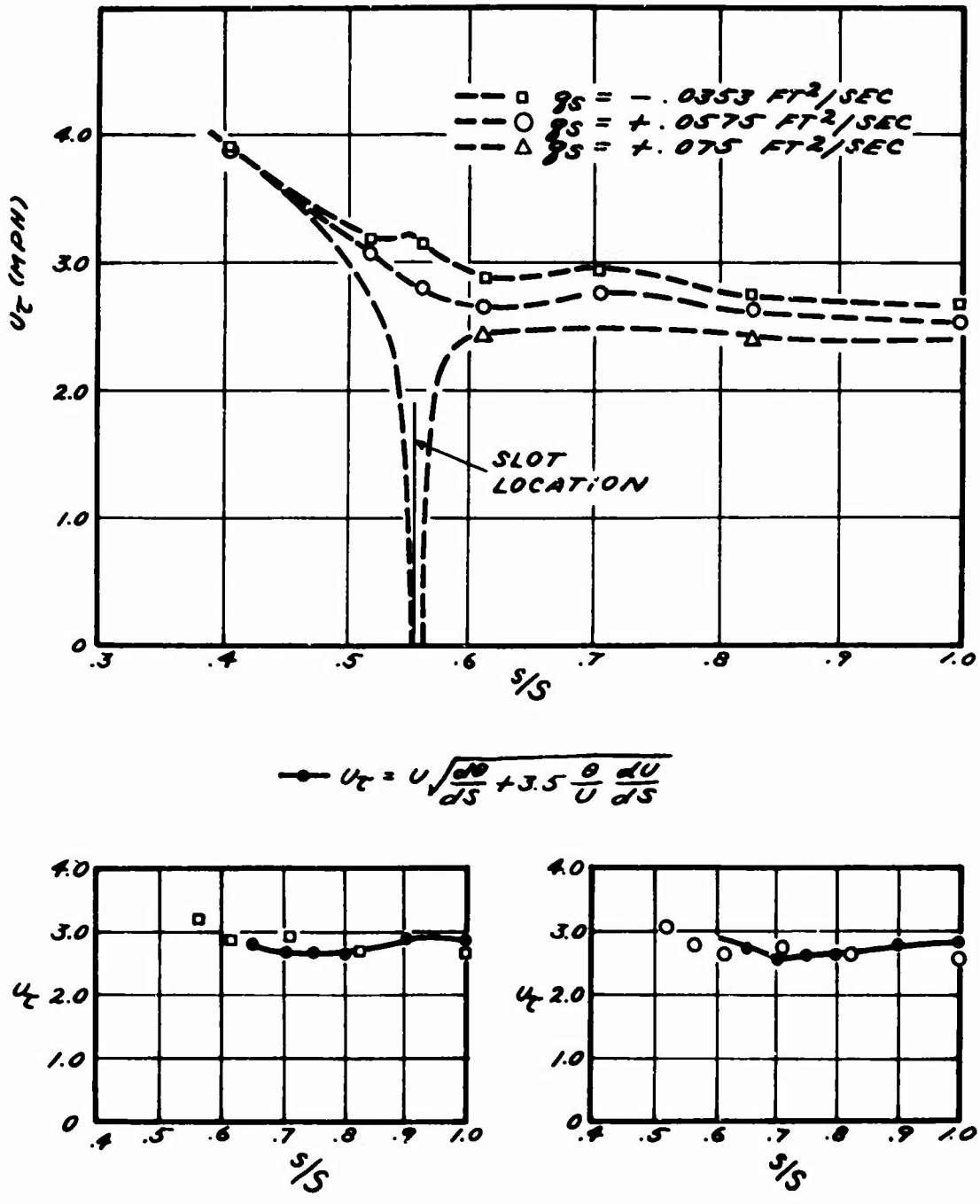

Figure 23. Effect of Transpiration on Friction Velocity U_τ in Case of the 90° Slot.

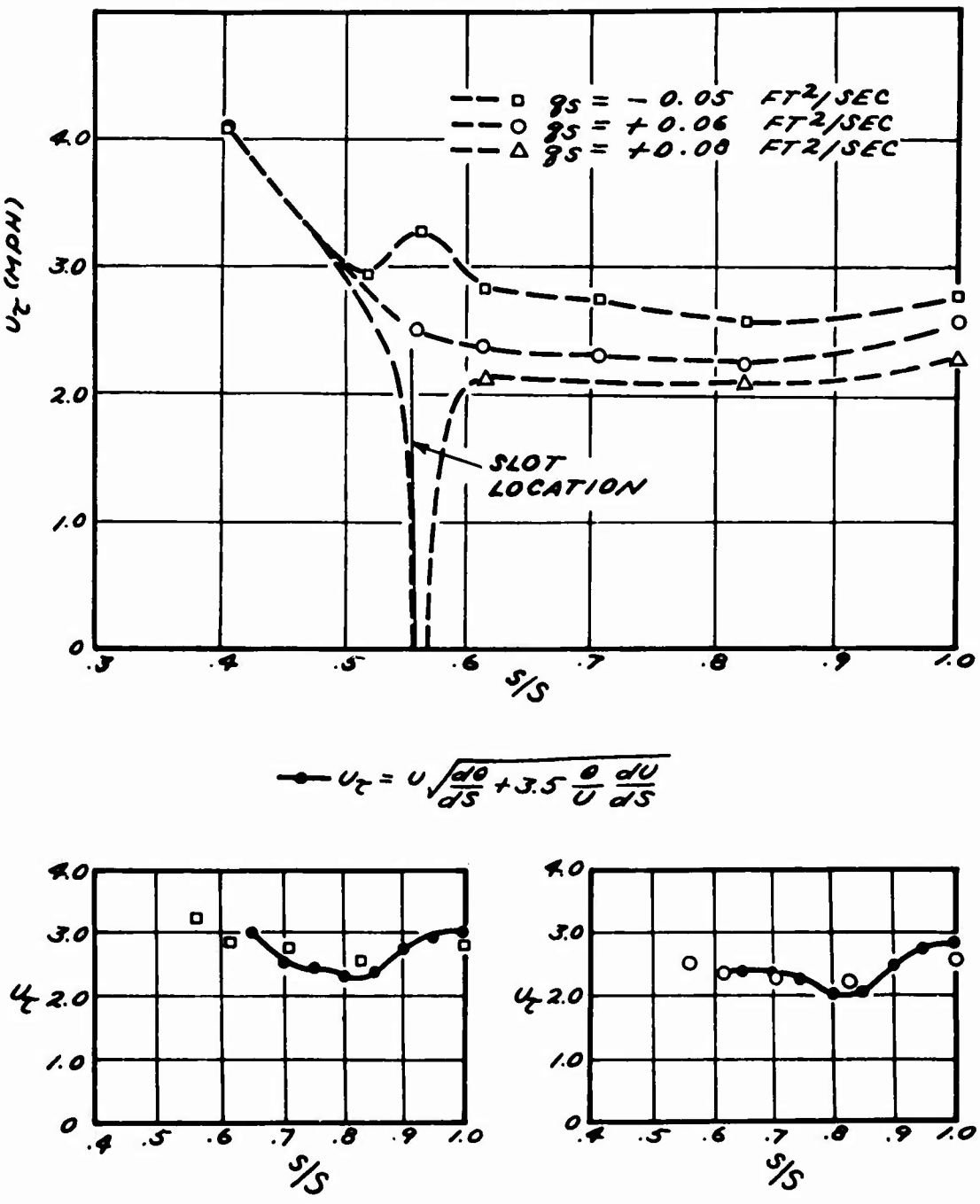

Figure 24. Effect of Transpiration on Friction Velocity U_τ in Case of the 135° Slot.

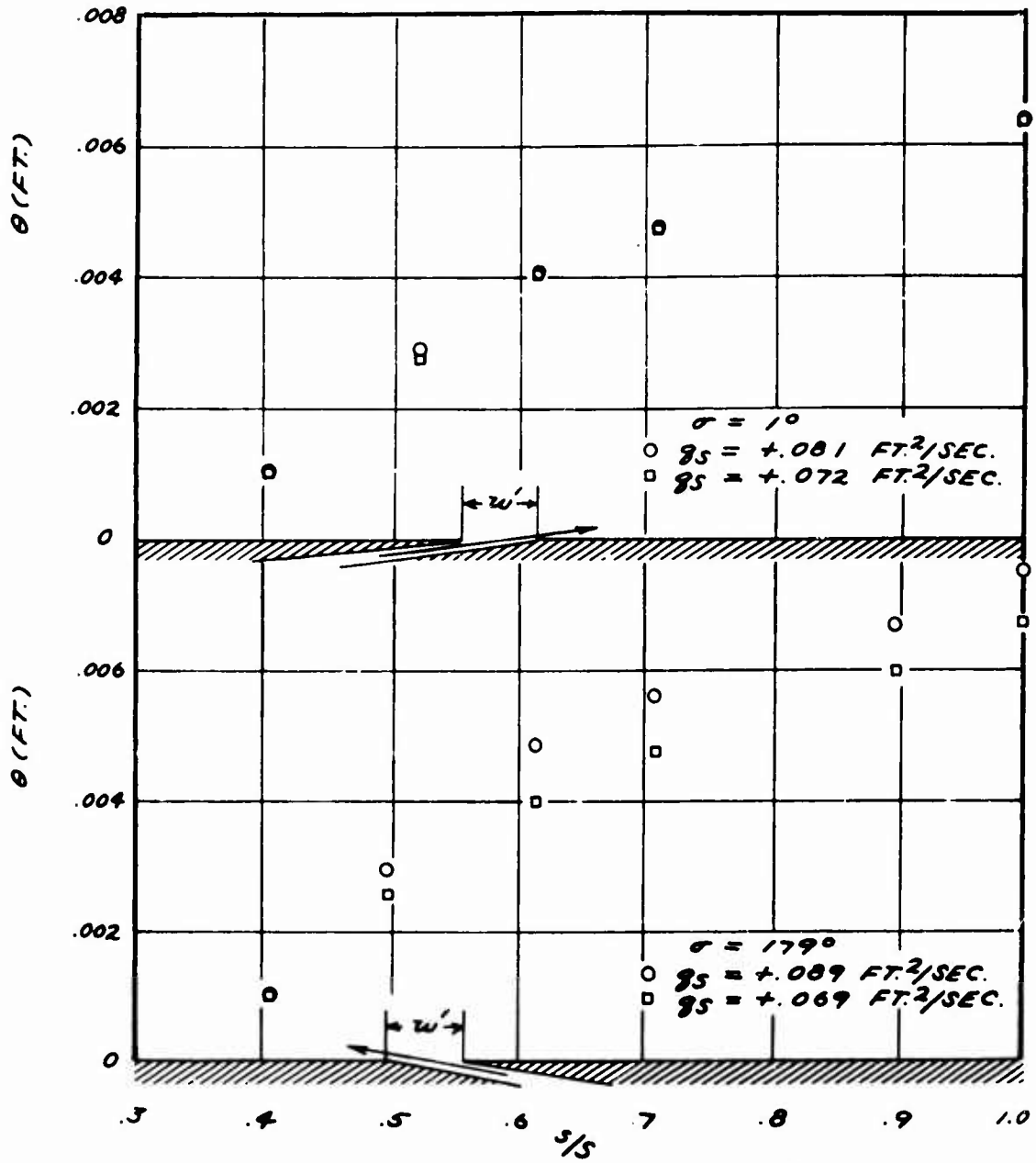

Figure 25. Effect of Injection on Momentum Loss Thickness at Extreme Slot Angles.

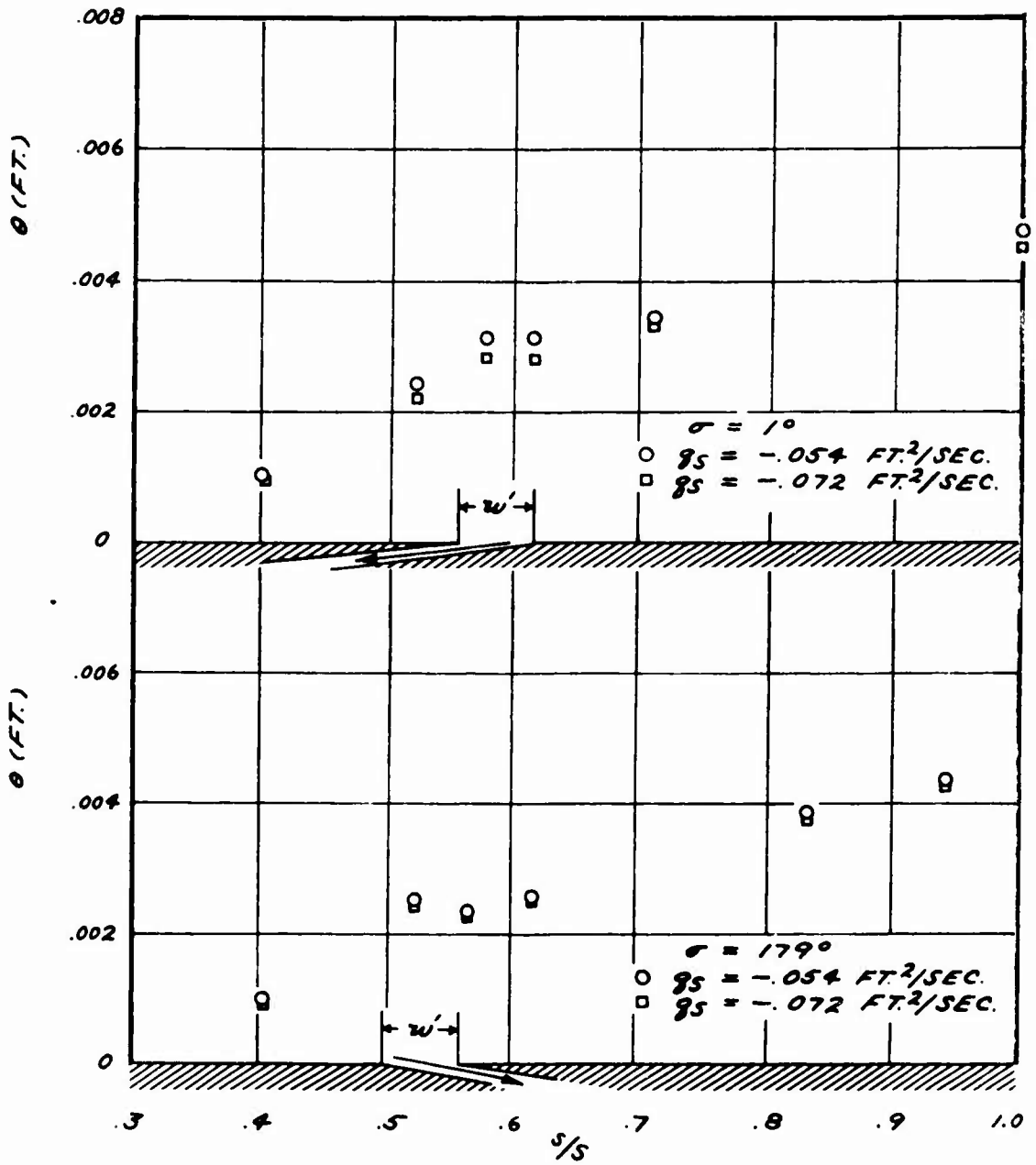

Figure 26. Effect of Suction on Momentum Loss Thickness at Extreme Slot Angles.

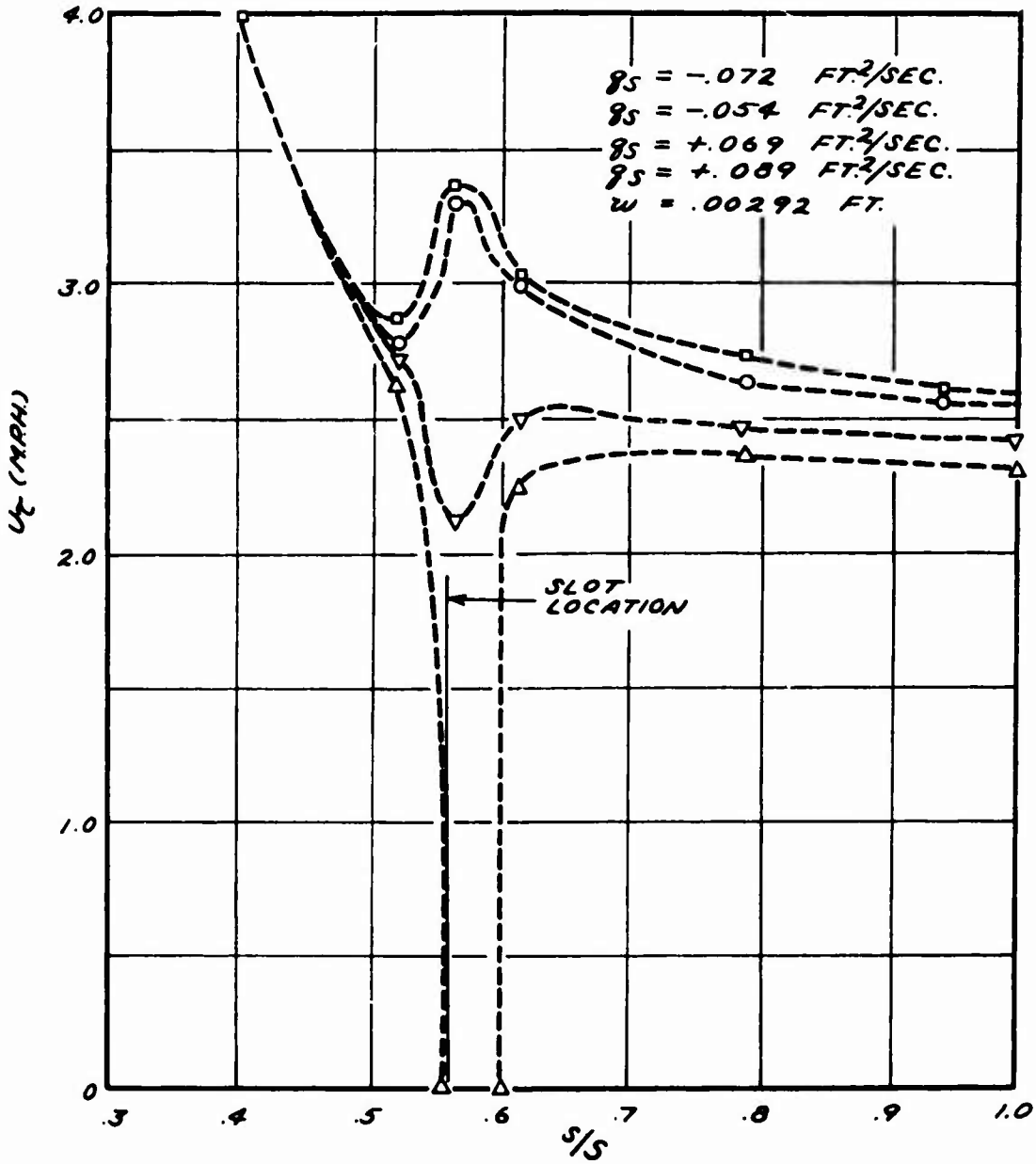

Figure 27. Effect of Transpiration on Friction Velocity U_τ in Case of 179° Slot.

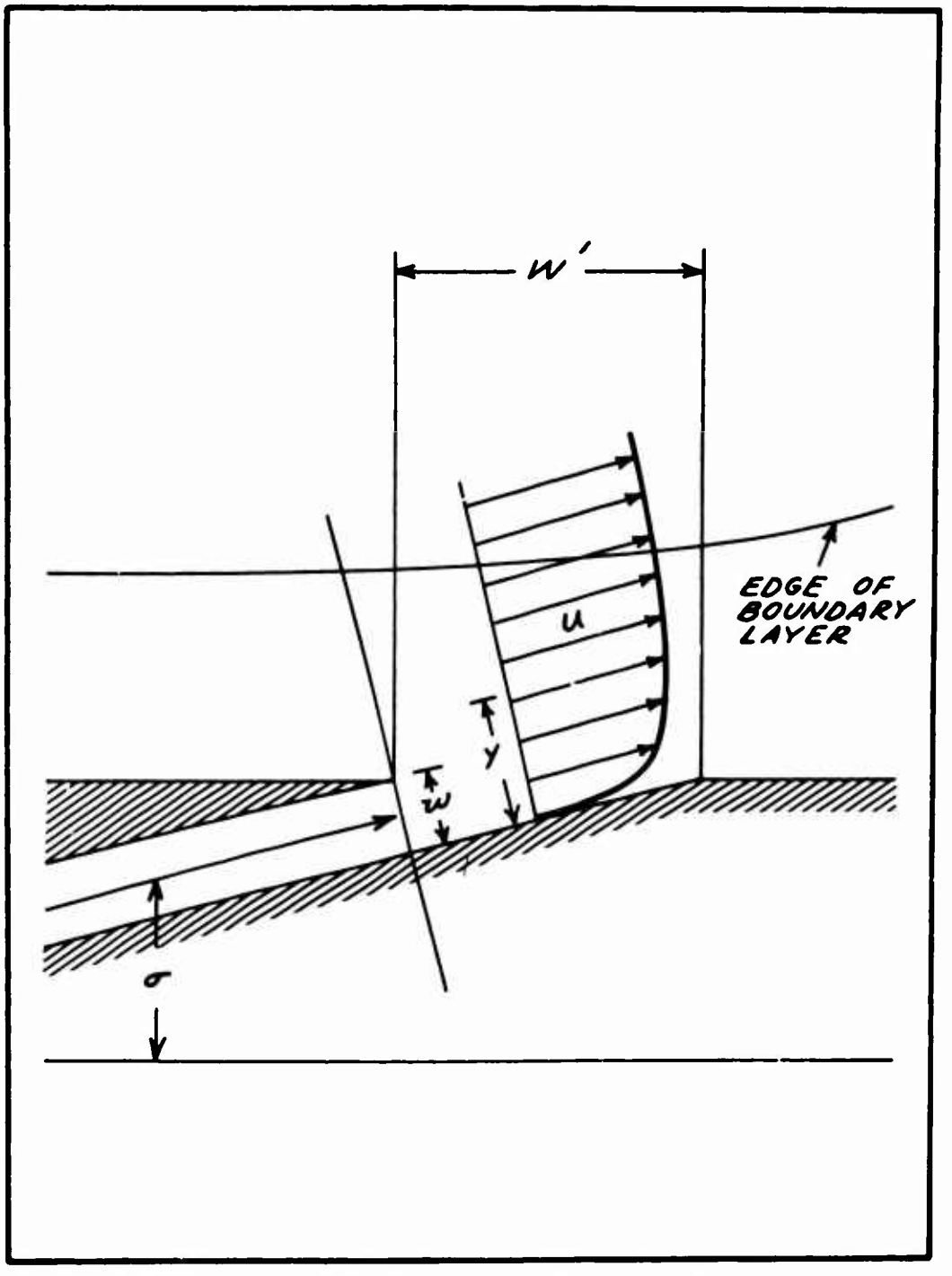

Figure 28. Diagram of Conditions Existing in Vicinity of Extreme Angled Slot.

DISTRIBUTION

U. S. Army Materiel Command	1
U. S. Army Mobility Command	3
U. S. Army Aviation Materiel Command	2
Chief of R&D, D/A	1
U. S. Army Transportation Research Command	22
U. S. Army Research and Development Group (Europe)	2
U. S. Army Engineer Research and Development Laboratories	3
Army Research Office-Durham	1
U. S. Army Engineer Waterways Experiment Station	1
U. S. Army Combat Developments Command Aviation Agency	1
Air University Library, Maxwell AFB	1
Bureau of Naval Weapons	1
David Taylor Model Basin	1
Ames Research Center, NASA	1
NASA-LRC, Langley Station	1
Lewis Research Center, NASA	1
NASA Representative, Scientific and Technical Information Facility	2
Research Analysis Corporation	1
National Aviation Facilities Experimental Center	1
U. S. Army Standardization Group, Canada	1
Canadian Liaison Officer, U. S. Army Transportation School	1
British Army Staff, British Embassy	1
U. S. Army Standardization Group, U. K.	1
Defense Documentation Center	10
U. S. Government Printing Office	1
Marine Corps Liaison Officer, U. S. Army Transportation School	1

Mississippi State University, Aerophysics Department, State College, Mississippi, EFFECTS OF TRANSPIRATION THROUGH ANGLED SLOTS ON THE DEVELOPMENT OF THE TURBULENT BOUNDARY LAYER - Gordon Leonard Harris, Research Report No. 43, TRECOM Technical Report 64-43, September 1964, 44 pp., (Contract DA 44-177-AMC-892(T)) USATRECOM Task 1D121401A14203.

Unclassified Report

In this study an attempt was made to fundamentally understand the nature of slot transpiration and to establish

(over)

1. Blown Slots
2. Contract DA 44-177-AMC-892(T)

Mississippi State University, Aerophysics Department, State College, Mississippi, EFFECTS OF TRANSPIRATION THROUGH ANGLED SLOTS ON THE DEVELOPMENT OF THE TURBULENT BOUNDARY LAYER - Gordon Leonard Harris, Research Report No. 43, TRECOM Technical Report 64-43, September 1964, 44 pp., (Contract DA 44-177-AMC-892(T)) USATRECOM Task 1D121401A14203.

Unclassified Report

In this study an attempt was made to fundamentally understand the nature of slot transpiration and to establish

(over)

1. Blown Slots
2. Contract DA 44-177-AMC-892(T)

Mississippi State University, Aerophysics Department, State College, Mississippi, EFFECTS OF TRANSPIRATION THROUGH ANGLED SLOTS ON THE DEVELOPMENT OF THE TURBULENT BOUNDARY LAYER - Gordon Leonard Harris, Research Report No. 43, TRECOM Technical Report 64-43, September 1964, 44 pp., (Contract DA 44-177-AMC-892(T)) USATRECOM Task 1D121401A14203.

Unclassified Report

In this study an attempt was made to fundamentally understand the nature of slot transpiration and to establish

(over)

1. Blown Slots
2. Contract DA 44-177-AMC-892(T)

Mississippi State University, Aerophysics Department, State College, Mississippi, EFFECTS OF TRANSPIRATION THROUGH ANGLED SLOTS ON THE DEVELOPMENT OF THE TURBULENT BOUNDARY LAYER - Gordon Leonard Harris, Research Report No. 43, TRECOM Technical Report 64-43, September 1964, 44 pp., (Contract DA 44-177-AMC-892(T)) USATRECOM Task 1D121401A14203.

Unclassified Report

In this study an attempt was made to fundamentally understand the nature of slot transpiration and to establish

(over)

1. Blown Slots
2. Contract DA 44-177-AMC-892(T)

an appropriate mathematical formulation of the problem suitable for solution. The theoretical solutions were compared with experimental data obtained at Flight Reynolds numbers.

The experimental data indicates that the theoretical methods are capable of predicting the effect of transpiration through angled slots on the development of the momentum loss thickness of a turbulent boundary layer with the condition that separation does not occur at the downstream edge of the slot.

an appropriate mathematical formulation of the problem suitable for solution. The theoretical solutions were compared with experimental data obtained at Flight Reynolds numbers.

The experimental data indicates that the theoretical methods are capable of predicting the effect of transpiration through angled slots on the development of the momentum loss thickness of a turbulent boundary layer with the condition that separation does not occur at the downstream edge of the slot.

an appropriate mathematical formulation of the problem suitable for solution. The theoretical solutions were compared with experimental data obtained at Flight Reynolds numbers.

The experimental data indicates that the theoretical methods are capable of predicting the effect of transpiration through angled slots on the development of the momentum loss thickness of turbulent boundary layer with the condition that separation does not occur at the downstream edge of the slot.

an appropriate mathematical formulation of the problem suitable for solution. The theoretical solutions were compared with experimental data obtained at Flight Reynolds numbers.

The experimental data indicates that the theoretical methods are capable of predicting the effect of transpiration through angled slots on the development of the momentum loss thickness of turbulent boundary layer with the condition that separation does not occur at the downstream edge of the slot.